Imperial College London
Department of Physics

Observational Constraints on the Dark Energy Equation of State

Florian W Borchers

September 10, 2010

Supervised by Dr Contaldi

Submitted in part fulfilment of the requirements for the degree of
Master of Science in Physics of Imperial College London

Declaration

I herewith certify that all material in this dissertation which is not my own work has been properly acknowledged.

Florian W Borchers

Abstract

Modern cosmology is based on the two pillars of homogeneity and isotropy. In apparent violation of these principles we observe prominent structures in the CMB and in the galaxy distribution. Here we show how they find their natural explanation in perturbations around the homogeneous background. Both, radiation and matter perturbations are supposedly set during inflation. The most convincing suggestions contain perturbations that started off as quantum fluctuations and were inflated in the process of the rapid expansion of the universe. At the end of inflation they reached a cosmological size large enough to act as initial seed for the perturbations we observe.

We discuss the evolution of the small perturbations at the end of inflation to the highly nonlinear matter perturbations today. We use a perturbed metric from general relativity to describe the gravitational potential and a relativistic Boltzmann system to deal with the interactions of the perturbations. It proves very helpful to do this in Fourier space instead of real space. We insert the equations into a computer and compare the numerical results with analytical approximations where they exist. This interplay lets us confidentially come to the conclusion that the growth of the matter perturbations is suppressed during radiation domination. Only after radiation-matter equality the perturbations have opportunity to grow substantially. During the long matter dominated era before effects of dark energy become important the perturbations reach the size consistent with observations.

A very important means to compare theoretical predictions with observations is the power spectrum, because radiation, matter and dark energy leave their signatures in the power spectrum. We compare the predictions for the power spectrum of a model of the universe without dark energy with a model with dark energy and come to the conclusion that the theory of perturbations favours a model with dark energy

Contents

List of Figures

1. The Homogeneous Universe

1.1. Introduction

Today cosmology has a standard model. The underlying principles of modern cosmology are homogeneity and isotropy. *Homogeneity* implies that the universe has the same properties everywhere in space. This is obviously false when we think of all the structures on earth, the solar system and the galaxy. When we go to larger and larger structures, however, homogeneity takes over: averaging over large patches of the universe containing several clusters of galaxies, i.e. averaging over sufficiently large scales leaves a highly homogeneous background. It is this background that is supposed to be homogeneous.

Isotropy of the universe means the universe looks the same in every direction. Again, this is evidently false in our neighbourhood, as the galaxy distribution that we observe is highly anisotropic. The further we look, however, the more isotropic the universe becomes. The cosmic microwave background is surprisingly isotropic.

The principles of homogeneity and isotropy imply two important consequences: The position of the earth in the universe cannot be special, because that would violate homogeneity. Secondly, any other centre of the universe cannot exist either. This is, in a sense, a modern version of the Copernican principle.

Cosmology is concerned with the physics of the whole universe. Averaging over small scales implies, fortunately for the physicist, that only gravity has to be considered. All other fundamental forces (electromagnetic, strong, weak) are either confined to the scales of particle physics or the charges are aligned to charge-neutral objects. Neither of these effects happen to gravity. That is why cosmology applies the theoretical description of gravity, general relativity, to the universe. The four dimensional spacetime of the universe is highly curved, which is manifest in the expansion of the three dimensional subspace, the real space.

The first chapter of this thesis will be summarising how physics describes the homogeneous background of the universe and how this results from general relativity. At the end of this chapter we give a very short introduction of what the presence of dark energy changes. The second chapter is an extensive discussion of

the matter perturbations and their evolution throughout the universe. We compare analytic expectations to numerical data. Chapter 3 deals with the effects of dark energy at late times on the matter perturbations, whereas chapter 4 shortly discusses the differences between a cosmological constant and dark energy as a more general approach.

1.2. The Expansion of the universe

We will use $c = 1$ and $\hbar = 1$ throughout this document as it is usual for theoretical physics. General Relativity says that the metric of a homogeneous and isotropic universe is of the form

$$ds^2 = g_{\mu\nu} dx^\mu dx^\nu \tag{1.1}$$

(summed over the indices μ and ν from 0 to 3 following the Einstein summation convention here and in the following), where the metric tensor takes the form

$$g_{\mu\nu} = \begin{pmatrix} -1 & 0 & 0 & 0 \\ 0 & a^2(t) & 0 & 0 \\ 0 & 0 & a^2(t) & 0 \\ 0 & 0 & 0 & a^2(t) \end{pmatrix} \tag{1.2}$$

which is called a Friedmann-Robertson-Walker (FRW) metric. The time variable a is called the scale factor and turns out very helpful in the discussion of the expansion of the universe (see below).

The principle of general relativity that particles follow locally straight lines is translated into the geodesic equation:

$$\frac{D^2 x^\mu}{d\lambda^2} = 0, \tag{1.3}$$

where D stands for covariant differential and λ is the proper time τ (for massive particles) or some parameter used to describe the orbit (in case of a massless particle). Writing this equation in usual differentials the geodesic equation becomes

$$\frac{d^2 x^\mu}{d\lambda^2} = -\Gamma^\mu_{\rho\sigma} \frac{dx^\rho}{d\lambda} \frac{dx^\sigma}{d\lambda}, \tag{1.4}$$

where Γ denotes the Christoffel symbols of the FRW metric.

The equation that relates the metric to the content of the spacetime is Einstein's

field equation. First, we need to introduce the Einstein tensor

$$G_{\mu\nu} := R_{\mu\nu} + \frac{R}{2} g_{\mu\nu}, \tag{1.5}$$

where $R_{\mu\nu}$ is the Ricci tensor and R is its trace. The field equation then takes the form

$$G_{\mu\nu} = 8\pi G\, T_{\mu\nu} + \Lambda g_{\mu\nu}, \tag{1.6}$$

which relates the Einstein tensor $G_{\mu\nu}$ to the content of the universe, i.e. all sorts of particles (summed together to the energy-momentum tensor $T_{\mu\nu}$) and cosmological constant Λ.

Going through the calculations two equations for the scale factor $a(t)$ are obtained. These so called Friedmann equations describe the expansion of the universe:

$$\left(\frac{\dot{a}}{a}\right)^2 = \frac{8\pi G}{3}\rho(t) - \frac{k}{a^2} + \frac{\Lambda}{3} \tag{1.7}$$

$$\frac{\ddot{a}}{a} = -\frac{4\pi G}{3}\left(\rho(t) + 3p(t)\right) + \frac{\Lambda}{3} \tag{1.8}$$

The newly introduced parameters are the curvature in the three dimensional subspace k, the mean density of matter in the universe $\rho(t)$ and its pressure $p(t)$. Λ denotes the cosmological constant or dark energy implemented as cosmological constant. Fig. 1.1 shows the evolution of the scale factor a with cosmic time t for a universe that starts off radiation dominated. At some point matter becomes the driving force behind the expansion and the slope of the double-logarithmic plot changes indicating the time of radiation-matter equality.

The Hubble rate $H(t)$ is a measure for the change of the scale factor $a(t)$. Its definition is given by

$$H(t) = \frac{da/dt}{a(t)}. \tag{1.9}$$

Today's value for H is denoted as $H_0 = H(t = \text{today})$[1]. It is often written in another parameter h[2] via

$$H_0 = 100\, h\, \mathrm{km}\, s^{-1}\, \mathrm{Mpc}^{-1} \tag{1.10}$$

[1] Here and in the following we will use the subscript 0 to indicate today's value of a variable.

[2] Due to this occurrence of h we will never use the letter for Planck's constant, which is set to be equal to one: $\hbar = 1$.

with $h \approx 0.72 \pm 0.08$ as best value today. It defines the critical density via

$$\rho_{\rm cr} = \frac{3H_0^2}{8\pi G}, \tag{1.11}$$

$$\rho_{\rm cr0} \approx 1.88\, h^2 \times 10^{-33} {\rm kg\,m^{-3}}, \tag{1.12}$$

where the last line gives the numerical value for today's critical density.

The conservation of the energy momentum tensor $T_{\mu\nu}$ gives a conservation equation:

$$\frac{DT_{\mu\nu}}{dx^\mu} = 0 \qquad \Rightarrow \qquad \frac{\partial \rho}{\partial t} + \frac{\dot{a}}{a}[3\rho + 3p] = 0. \tag{1.13}$$

Pressure and density of the particles in the universe are connected via the equation of state $p = w\rho$ with parameter w. Most common are:

$$\text{dust (matter):} \qquad w_m = 0 \qquad p = 0 \tag{1.14}$$

$$\text{radiation:} \qquad w_\gamma = \frac{1}{3} \qquad p = \frac{1}{3}\rho \tag{1.15}$$

$$\text{dark energy:} \qquad w_{\rm DE} = -1 \qquad p = -\rho \tag{1.16}$$

Matter – be it dark matter, baryons or electrons – is largely pressureless, because its kinetic energy is much smaller then its rest energy with which it needs to be compared with. It is therefore generally described as *dust*. Photons, however, are relativistic particles in equilibrium with the temperature. Therefore they have $w = 1/3$. The equation of state parameter of the dark energy is of interest to current research. If dark energy indeed behaves like a cosmological constant, its parameter is $w = -1$.

Using the expression for the pressure we can substitute p in the conservation equation, Eq. (1.13). In case of only one type of content (or a dominating type) the conservation equation can be integrated to

$$\text{dust:} \qquad \rho_m a^3 = \text{const} \tag{1.17}$$

$$\text{radiation} \qquad \rho_\gamma a^4 = \text{const} \tag{1.18}$$

$$\text{dark energy:} \qquad \rho_{\rm DE} = \frac{\Lambda}{3}\frac{1}{H_0^2}\rho_{\rm cr} = \text{const.} \tag{1.19}$$

In the following discussion of the homogeneous universe we will assume the evolution of the different species of particles is independent from each other. This means the different evolution equations above are valid for each species. It is then feasible to parametrize the contribution of the species by their value today. Using

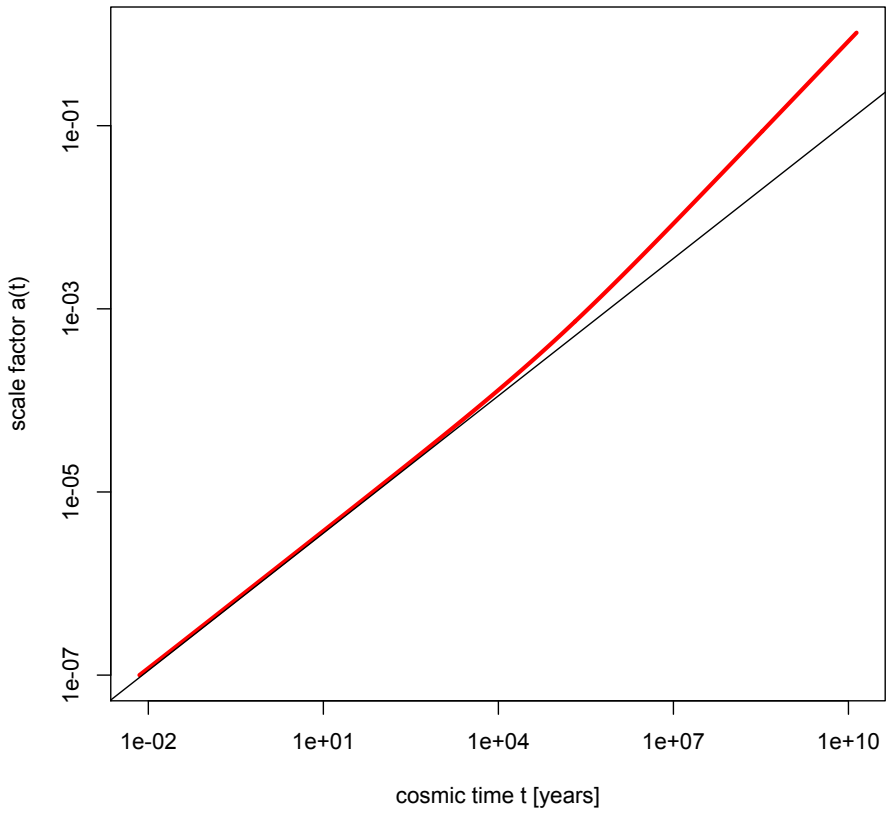

Figure 1.1.: Scale factor $a(t)$ versus cosmic time t (thick line). The growth of the scale factor depends on the dominating content of the universe. In early times, during radiation domination it grows as $t^{1/2}$ (c.f. the linear approximation with the thin line), later, during matter domination it grows as $t^{2/3}$. We see a clear departure from the radiation approximation. This agrees with Fig. 1.2 in Dodelson[5].

the critical density $\rho_{\rm cr}$ defined above we introduce the dimensionless parameters

$$\Omega_i(t) := \frac{\rho_i(t)}{\rho_{\rm cr}(t)}, \quad i = \mathrm{m}, \gamma, \mathrm{etc.} \tag{1.20}$$

Fig. 1.3 shows the contribution of the different types of content to the critical density at various times. The different eras of the evolution of the universe can be clearly distinguished by the change in Ω_i. The universe starts radiation dominated, but matter takes over not lang after. In late times the universe is supposed to be dominated by dark energy, here as cosmological constant.

Using the new parameters, the Hubble rate H and the Ω_i the Friedmann equation, Eq. (1.7), can be written as

$$H^2(t) = H_0^2(\Omega_\gamma a^{-4} + \Omega_m a^{-3} + \Omega_k a^{-2} + \Omega_{\rm DE}) \tag{1.21}$$

when setting $\Omega_k := k$.

1.3. Temperature, the CMB and other photons

Referring to the temperature of the universe usually means the temperature of the photons, which we today measure as the cosmic microwave background (CMB). There have been many experiments and satellites measuring this temperature, its best value today is $T_0 = 2.725 \pm 0.002K$ (Mather et al., 1999). The microwave photons we observe are very well described by black body radiation with this temperature.

Because the energy of a photon is determined by its wavelength and the wavelength is stretched by the expansion of the universe the energy density of the photons drops off with with ageing universe as

$$T(t) = \frac{T_0}{a(t)}. \tag{1.22}$$

This means that when we observe photons today with wavelength $\lambda_{\rm obs}$ they had a much shorter wavelength when they were emitted: $\lambda_{\rm emit}$. To quantify this change we define the redshift z via:

$$1 + z := \frac{\lambda_{\rm obs}}{\lambda_{\rm emit}} = \frac{1}{a(t)}. \tag{1.23}$$

In an expanding universe we see everything (i.e. galaxies, as only these objects are bright enough to be detected over large enough distances) recede from our

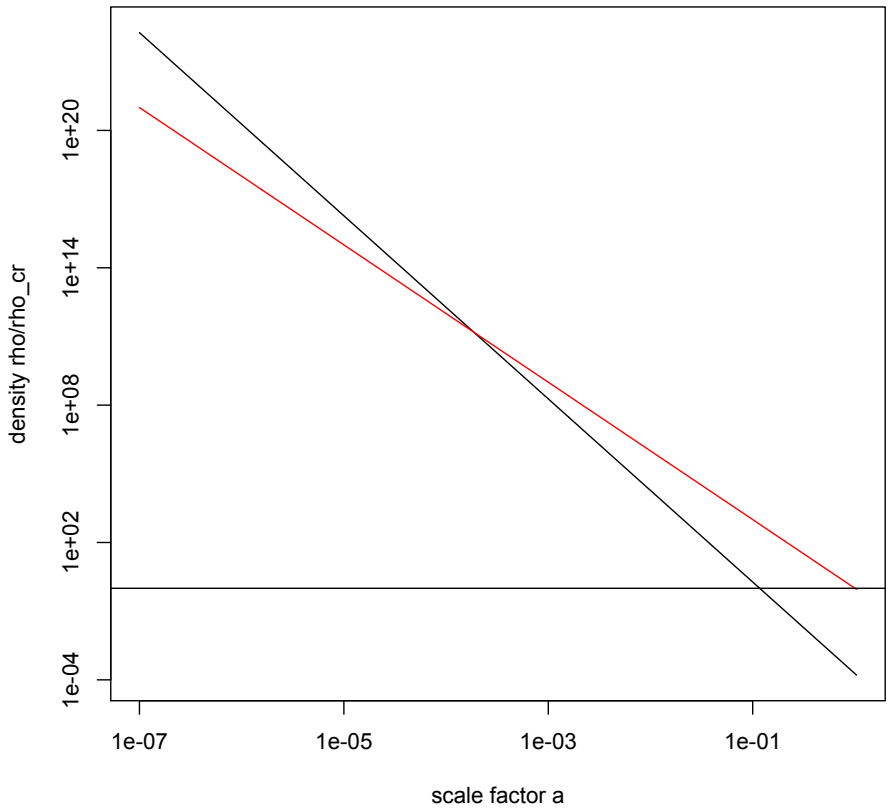

Figure 1.2.: This plot shows the radiation and matter densities in the homogeneous universe in a double logarithmic plot. The different slopes of radiation and matter correspond to the different exponents in Eq. (1.17) and the following. The density of a cosmological constant is the same throughout the ages. When radiation and matter have the same contribution to the critical density of the universe we speak of radiation-matter equality. This agrees with Fig. 1.3 in Dodelson[5].

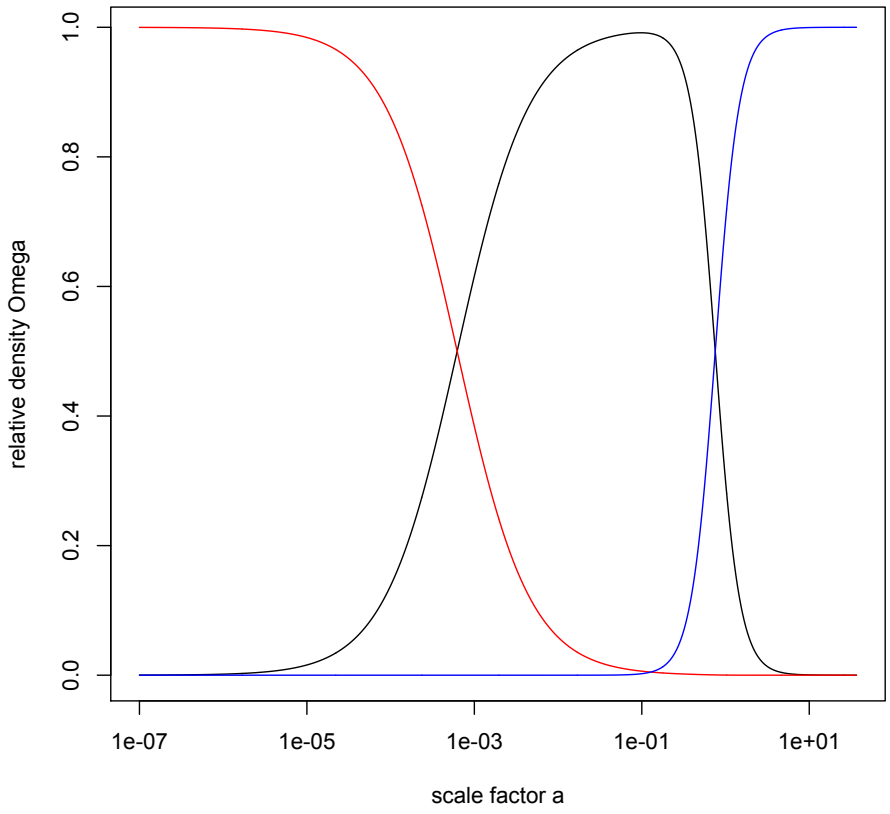

Figure 1.3.: Relative density of the content in the universe plotted against scale factor $a(t)$. At early times the radiation is by far the driving force (radiation dominated universe), but it falls off rather rapidly. Matter takes over at radiation-matter equality (matter dominated universe). At late time the universe is dominated by dark energy

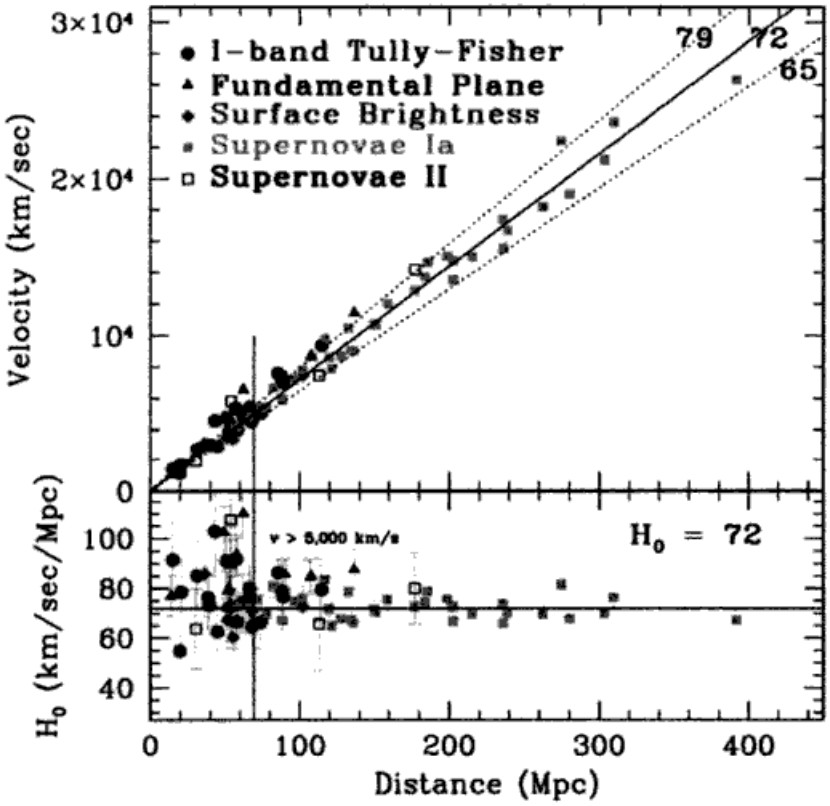

Figure 1.4.: This is the Hubble diagram published by the Hubble Space Telescope (HST) Key Project, [7]. It shows the receding velocities of objects in our intergalactic neighbourhood. Data are derived from various methods including the use of the Tully-Fisher relation and supernovae data as standard candles. The lower panel shows the residues from the best fit for today's Hubble rate: The note $H_0 = 72$ implies $h = 72$ in our notation.

position, just as any other observer in the universe. This observation was first made by Edwin Hubble in 1929 and the corresponding diagram, Fig. 1.4 was named after him.

1.4. Conformal Time η

Just as time, scale factor or temperature we can use conformal time η to parametrize the evolution of the universe. Its definition is given by

$$\eta := \int_0^t \frac{dt'}{a(t')}. \tag{1.24}$$

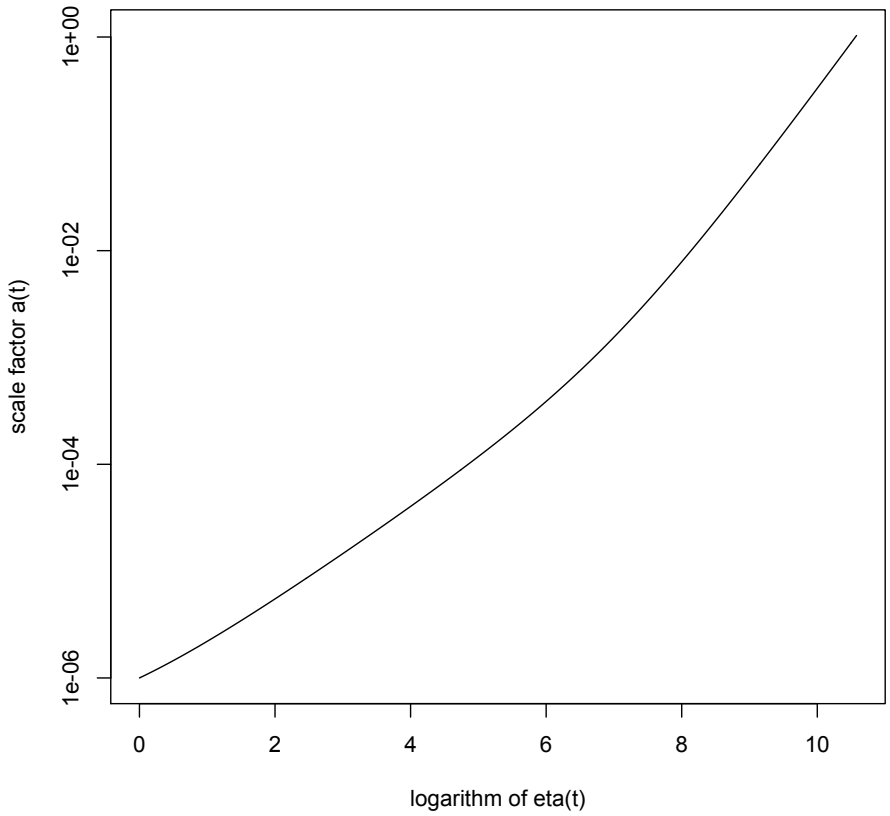

Figure 1.5.: The scale factor a is plotted versus conformal time η. During radiation dominated epoch the scale factor is proportional to η, in matter dominated epoch it is proportional to η^2.

When the universe is dominated by one type of content there exist analytical expressions for η: During radiation domination a grows as η, during matter domination, however, a grows as η^2.

Proof. From the definition of η we see that

$$\frac{d\eta}{dt} = \frac{1}{a(t)}. \tag{1.25}$$

During radiation domination we have $a \propto \sqrt{t}$ s.t.

$$\eta = \int d\eta \propto \int \frac{dt}{\sqrt{t}} \propto \sqrt{t} \propto a, \tag{1.26}$$

whereas in matter domination we have $a \propto t^{2/3}$ which leads to

$$\eta = \int d\eta \propto \int \frac{dt}{t^{2/3}} \propto t^{1/3} \propto \sqrt{a}. \tag{1.27}$$

These relations proof the claim. □

In a universe with radiation and matter only, the evolution of η with the scale factor $a(t)$ is given by:

$$\eta = \frac{2}{\sqrt{\Omega_m H_0^2}} \left(\sqrt{a + a_{\mathrm{eq}}} - \sqrt{a_{\mathrm{eq}}} \right) \tag{1.28}$$

Proof. In a radiation and matter dominated universe the Friedmann equation becomes

$$H^2(t) = H_0^2(\Omega_r a^{-4} + \Omega_m a^{-3}). \tag{1.29}$$

The scale factor a_{eq} at the time of radiation matter equality is given by the equation $\Omega_r a_{\mathrm{eq}}^{-4} = \Omega_m a_{\mathrm{eq}}^{-3}$. We use this to replace the parameter Ω_r in favour of Ω_m. Rearranging the terms in the Friedmann equation and using $H = a^{-1} da/dt$ we find

$$\frac{da}{a} = H_0 \sqrt{\Omega_m} \sqrt{a_{\mathrm{eq}} a^{-2} + a^{-1}} \frac{dt}{a}. \tag{1.30}$$

This can be used to replace the integrand dt/a in the definition of η. We then find

$$\eta = \int_0^t \frac{dt'}{a(t')} = \int_0^{a(t)} \frac{1}{\sqrt{\Omega_m} H_0} \frac{da'}{\sqrt{a_{\mathrm{eq}} + a'}} \tag{1.31}$$

$$= \frac{2}{\sqrt{\Omega_m} H_0} \left(\sqrt{a(t) + a_{\mathrm{eq}}} - \sqrt{a_{\mathrm{eq}}} \right), \tag{1.32}$$

where the last line simply is the evaluation of the integral above. Thus we find the claim. □

Fig. 1.5 shows the evolution of the scale factor with conformal time η. In this double logarithmic plot the transition from radiation domination ($a \propto \eta$) to matter domination ($a \propto \eta^2$) is manifest in a changing gradient of the plotted line.

The usage of η instead of t will be very effective in the discussion of perturbations of the homogeneous universe, indeed, we will even change our notation from $\dot{(\,)} = d/dt$ to $\dot{(\,)} = d/d\eta$ in the next chapter.

1.5. Dark Energy

Today's data hint towards some kind of dark energy that is accelerating the expansion of the universe. The proposed origin of this phenomenon is being discussed in the literature today, suggestions range from a classical cosmological constant to a unified dark sector. Fig. 1.6 shows the supposed position of our universe in the $(\Omega_m, \Omega_\Lambda)$ parameter space. Observations suggest that it is not a flat matter dominated universe.

Because $\rho_L = \text{const}$ dark energy is bound to dominate the universe at late times. Fig. 1.7 is the analog of Fig. 1.1 with a cosmological constant dominant at late times. The scale factor grows immensely at this stage – here shown up to an age of 80 billion years – in accordance with the analytical exponential expectation for Λ domination:

$$a(t) \propto \exp(\sqrt{\Omega_\Lambda} H_0 t). \tag{1.33}$$

Proof. In a Λ dominated universe we write the Friedmann equation:

$$H^2(t) = H_0^2 \Omega_\Lambda \quad \Rightarrow \quad \frac{da}{dt} = H_0 \sqrt{\Omega_\Lambda} a(t). \tag{1.34}$$

This can be integrated by separation of the variables to give the claimed relation. □

Fig. 1.8 shows the plot corresponding to Fig. 1.5. Again, early in the universe first radiation, then matter dominate the Friedmann equation and the scale factor a grow correspondingly as η and then as η^2. However, as soon as the universe is dominated by the dark energy the scale factor grows exponentially in time. The integrand of η, however, $1/a(t)$ falls off very rapidly and the increment in η becomes negligible. This results in the steep rise in Fig. 1.8.

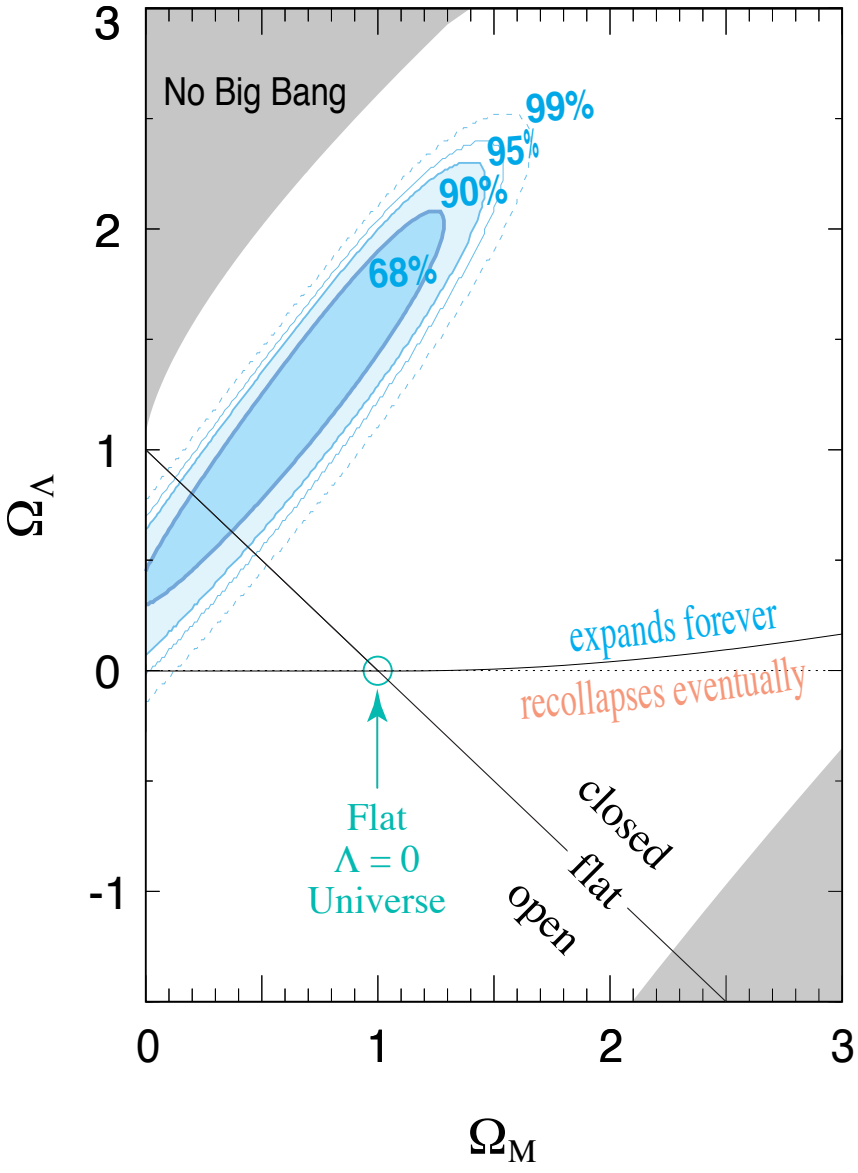

Figure 1.6.: In a plane of the parameters Ω_m and Ω_Λ the position of our universe is confined to the oval confidence levels obtained from supernovae observations. A flat, $\Lambda = 0$ universe clearly contradicts the observations, instead some kind of dark energy is favoured s.t. $\Omega_\Lambda \neq 0$. This figure is taken from [1].

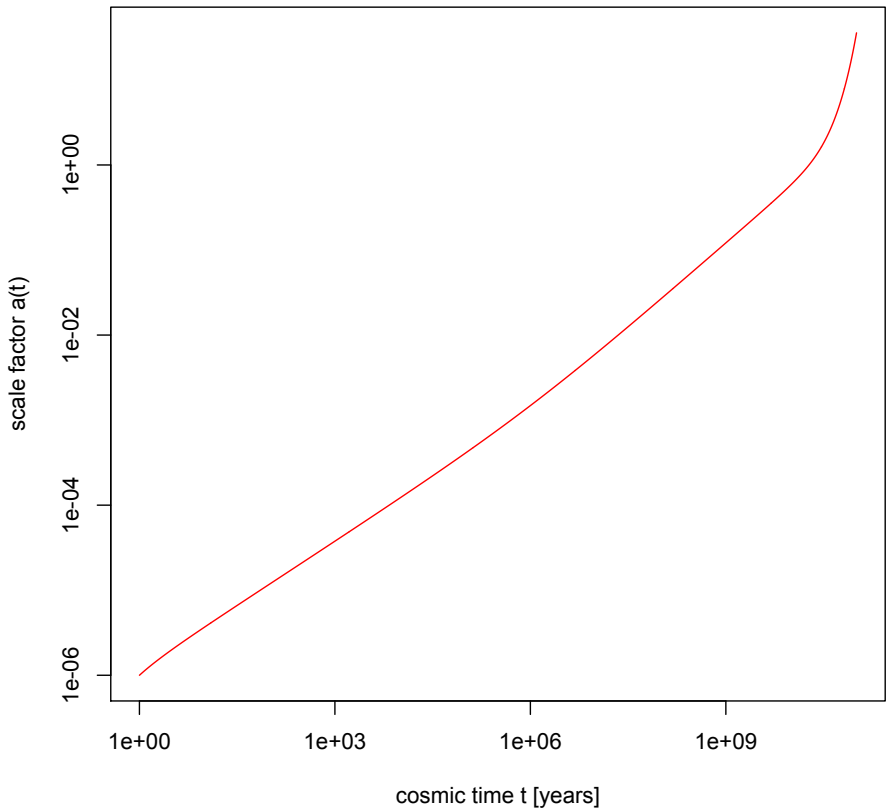

Figure 1.7.: This plot shows again scale factor $a(t)$ versus cosmic time t. In contrast to Fig. 1.1 there is a cosmological constant. It becomes important at late times when radiation and matter densities have fallen off. It drives the expansion exponentially.

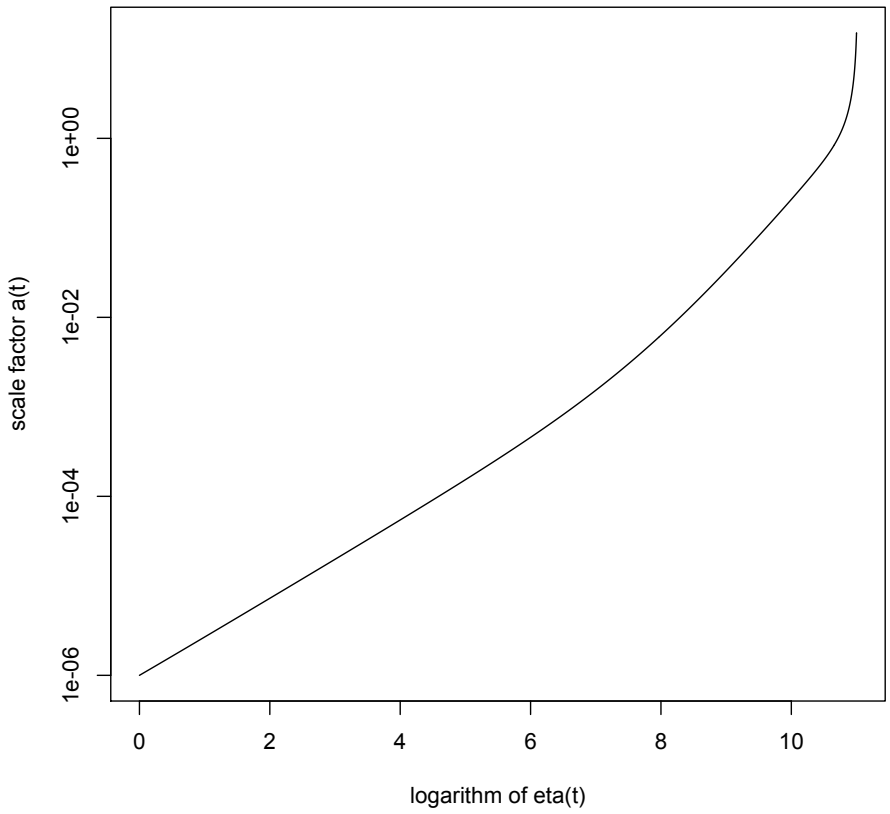

Figure 1.8.: Here the scale factor a is shown versus conformal time η. At late times dark energy becomes the dominating content of the universe. This is when the scale factor grows immensely with η.

2. Inhomogeneities in a Universe without Λ: $\Omega_m = 1$

The inhomogeneites in the universe today are supposed to have their origin in the primordial fluctuations of the universe set by inflation (or – in principle – by any other mechanism). The suggestion is that original inevitable quantum fluctuations were amplified by the inflationary phase to serve as the initial conditions for the growth of structures. For these initial conditions models usually predict a Gaussian random field with a matter power spectrum[1] of the form

$$P_\delta(k) = Ak^n, \qquad n \simeq 1, k = \|\mathbf{k}\|\,, \tag{2.1}$$

where $\mathbf{k}$ the wave vector, also referred to as mode number and A the amplitude. Both of these values need to be chosen in accordance with observations, from the CMB say. The power spectrum in principle gives the intensity of fluctuations on a given scale. The linear power spectrum above says that large-scale fluctuations are a lot less apparent then small-scale fluctuations. This is in accordance with our picture of the perturbations' origin in quantum fluctuations.

The important point is that the physics of the evolution of these inhomogeneities is well-understood, whereas their origin is a matter of current research. Hence, we will only discuss the former here.

Incidentally, as we are interested in explaining the distribution of galaxies today, the focus lies on the matter perturbations, i.e. both dark matter and baryons. Considering the fact that the baryonic fraction of the matter content of the universe is small compared to dark matter it seems to be a feasible assumption that baryons simply trace the evolution of the dark matter because of gravity. It is hence the fluctuations in the dark matter at the end of inflation that are the origin of today's matter fluctuations. These initial overdensities have a size of 1 in 10^5 in most models (compare standard texts on inflation). In the evolution of the universe there need to be processes that amplify these values enormously to explain the rich large-scale structure we observe today. To do so there is basically

[1] For definition and extensive discussion see 46

two ways: One is to find the underlying law of the physics of these processes, the other is to use a computer to simulate the evolution of n-bodies. The fundamental flaw with the former is that it can only describe linear perturbation theory. Non-linear effects can only be explained by comparison with simulated data.

The density contrast δ is used to describe the matter overdensities. Its definition is given by

$$\delta(\mathbf{x}, t) = \frac{\rho(\mathbf{x}, t) - \rho_{\mathrm{cr}}(t)}{\rho_{\mathrm{cr}}(t)}, \tag{2.2}$$

where $\rho(\mathbf{x}, t)$ is the density at a given point in spacetime and $\rho_{\mathrm{cr}}(t)$ the time-dependent critical density.

The basic form of the equation for δ is

$$\ddot{\delta} + (\text{pressure} - \text{gravity})\delta = 0, \tag{2.3}$$

where the overdot denotes the derivative with respect to time. Pressure tends to stop overdensities from growing, whereas gravity, of course, drags matter together. The growth rate of an overdense region in the universe is thus driven by the interplay of gravitational pull inwards and pressure pushing particles away from the region. In detail it is the full Boltzmann and Einstein systems that that have to replace this equation.

Boltzmann-Einstein System. Under these circumstances it is a valid approximation to ignore higher photon moments then monopole and dipole, and thus set the gravitational potentials $\Phi = -\Psi$ in the metric perturbations. In the notation used here the overdot represents differentiation with respect to $d/d\eta$, and we consider the Boltzmann-Einstein system in Fourier space: $\Theta_{r,0}$ radiation monopole, $\Theta_{r,1}$ radiation dipole, and v the velocities of the matter inhomogeneities. Note that we drop the notation of the density contrast, and let $\delta(k, \eta)$ denote the Fourier transform of the matter inhomogeneities from now on. The equations then read:

$$\dot{\Theta}_{r,0} + k\Theta_{r,1} = -\dot{\Phi} \tag{2.4}$$

$$\dot{\Theta}_{r,1} + \frac{k}{3}\Theta_{r,0} = \frac{-k}{3}\Phi \tag{2.5}$$

$$\dot{\delta} + ikv = -3\dot{\Phi} \tag{2.6}$$

$$\dot{v} + \frac{\dot{a}}{a}v = ik\Phi, \tag{2.7}$$

There is one more equation relating the potential Φ to the overdensities in

matter and radiation:

$$k^2\Phi + 3\frac{\dot{a}}{a}\left(\dot{\Phi} + \frac{\dot{a}}{a}\Phi\right) = 4\pi G a^2(\rho_{\rm dm}\delta + 4\rho_r\Theta_{r,0}). \tag{2.8}$$

An alternative to Eq. (2.8) is to use Eq. (5.81) in [5]:

$$k^2\Phi = 4\pi G a^2\left(\rho_{\rm dm}\delta + 4\rho_r\Theta_{r,0} + \frac{3aH}{k}(i\rho_{\rm dm}v + 4\rho_r\Theta_{r,1})\right), \tag{5.81}$$

with the advantage that this equation is an algebraic equation and not a differential equation.

Mode Number k. A mode is characterised by its mode number $\mathbf{k}$, or – equivalently – its wavelength $\lambda = 2\pi/\left\|\mathbf{k}\right\|$, where, of course, as above $k = \left\|\mathbf{k}\right\|$. Causal physics can only act on objects of the size of the Hubble horizon $1/aH$. As a manner of speaking we say a mode enters the horizon when its (fixed) wavelength becomes comparable to the (growing) Hubble horizon. Decisive for the development of a given mode is when it enters the horizon with respect to radiation-matter equality $a_{\rm eq}$. We define a relevant scale for modes that enter the horizon during radiation-matter equality via

$$k_{\rm eq} = a_{\rm eq}H(a_{\rm eq}) = \sqrt{\frac{2\Omega_m H_0^2}{a_{\rm eq}}} \tag{2.9}$$

$$= 0.073{\rm Mpc}^{-1}\,\Omega_m h^2. \tag{2.10}$$

Proof. To prove this simply insert the Friedmann equation and the corresponding numerical values for the parameter. □

Considering the fact that $a_{\rm eq} = 4.15\cdot 10^{-5}(\Omega_m h^2)^{-1}$ we will speak of large-scale modes if $k^{-1} \sim 1000h^{-1}$Mpc, which means they enter the horizon at $a \sim 0.03$, i.e. much later then radiation-matter equality.

2.1. Analytical Results

In Sec. 2.2 and the following we will discuss numerical results of these coupled differential equations. First, however, we will have opportunity to digress and discuss the analytical description of the processes. These exist for all modes entering in radiation or matter dominated era. No analytical description has been found for modes that enter during radiation-matter transition.

Super-horizon Evolution

Super-horizon indicates that the mode has not entered the horizon, but instead that its wavelength succeeds the Hubble horizon: $k\eta \ll 1$. In the early universe ($a = 10^{-7} - 10^{-6}$) this is true for all modes of physical interest. It implies that we can drop all k-dependent terms in the differential equations: The evolution is independent of mode number k, they all evolve identically. Early in the universe the potential Φ is then constant for all modes.

Proof. First, we note that the full Bolzmann-Einstein system, Eq. (2.4)-(2.8) simplifies to three equations as the velocities v and the dipole moment $\Theta_{r,1}$ decouple from the other equations. The system becomes

$$\dot{\Theta}_{r,0} = -\dot{\Phi} \tag{2.11}$$

$$\dot{\delta} = -3\dot{\Phi} \tag{2.12}$$

$$3\frac{\dot{a}}{a}\left(\dot{\Phi} + \frac{\dot{a}}{a}\Phi\right) = 4\pi G a^2(\rho_{\mathrm{dm}}\delta + 4\rho_r\Theta_{r,0}). \tag{2.13}$$

It can then be shown that for super-horizon modes the potential Φ obeys the following second order differential equation with respect to variable $y := a/a_{\mathrm{eq}}$:

$$\frac{d^2\Phi}{dy^2} + \frac{d\Phi}{dy}\frac{21y^2 + 54y + 32}{2y(y+1)(3y+4)} + \frac{\Phi}{y(y+1)(3y+4)} = 0. \tag{2.14}$$

This differential equation can be integrated to

$$\Phi(y) = \frac{3\sqrt{1+y}}{4y^3}\,\Phi(y \approx 0) \cdot \int_{y' \approx 0}^{y} y'^2 \frac{3y' + 4}{(1+y')^{3/2}}\,dy' \tag{2.15}$$

$$= \frac{1}{10}\frac{\Phi(y \approx 0)}{y^3}\left(16\sqrt{1+y} + 9y^3 + 2y^2 - 8y - 16\right) \tag{2.16}$$

This means that in the early universe (when $y \ll 1$) all modes are super-horizon and they share the same constant potential $\Phi(y \approx 0)$. This can be seen in the top left corner of Fig. 2.1 below, where all modes start at the same potential and only gradually depart from it when they enter the horizon. □

This proof also shows that the evolution of δ is rather uninteresting as long as the mode stays outside the horizon: The differential equation for δ, Eq. (2.12), tells us with $\Phi = \text{const}$ that $\dot{\delta} = 0$. In early times the potential and the inhomogeneities stay constant. This behaviour can be seen in Fig. 2.2, where δ is plotted versus scale factor $a(t)$. At early times all modes are constant and only start to grow when they entered the horizon.

Furthermore, from the proof above we can deduce another important result: we can predict the evolution of large-scale modes that entered the horizon much later. For those modes the derived Eq. (2.16) is valid through all times and we can take the $(y \to \infty)$-limit. In that case the $9y^3$ term dominates and we find

$$\Phi \to \frac{9}{10} \cdot \Phi(y \approx 0). \tag{2.17}$$

Even on the largest scales the potential suffers a drop of 10% when the universe passes through radiation-matter equality. Again, this feature can be seen in Fig. 2.1, where the largest mode shown drops according to the result here. Smaller modes enter the horizon earlier and show a completely different behaviour. The result of the 9/10 drop will be used below in the definition of transfer and growth function.

Horizon Crossing

Matter Domination In the section above we have seen that the potential Φ remains constant as long as the mode has not entered the horizon, this is early in the universe. During radiation-matter transition even the largest modes suffer a 10% drop. Another analytical result regards modes that enter the horizon well after radiation-matter equality: The potential is constant during horizon crossing as long as the universe is matter dominated.

Proof. In the equations of the full Boltzmann-Einstein system we replace all densities by $\rho = \rho_m = \rho_{\mathrm{dm}}$. The equations simplify considerably and going through the algebra we find that the potential must obey a differential equation of the form

$$\alpha\ddot{\Phi} + \beta\dot{\Phi} = 0, \quad \alpha, \beta = \text{const.} \tag{2.18}$$

One solution to this equation is a constant potential $\Phi = \text{const}$, and by the initial conditions we see it is the solution to Eq. (2.18). □

Fig. 2.1 shows the constant potential at late times for three modes. The numerical results again confirm our understanding of the physics behind the evolution of the different modes.

With constant potential Φ the overdensities δ then grow as $\delta \propto a$.

Proof. The relevant differential equation for δ is different from Eq. (2.12), however, and we recall with Eq. (2.6) from the full system that:

$$\dot{\delta} + ikv = -3\dot{\Phi} \tag{2.6}$$

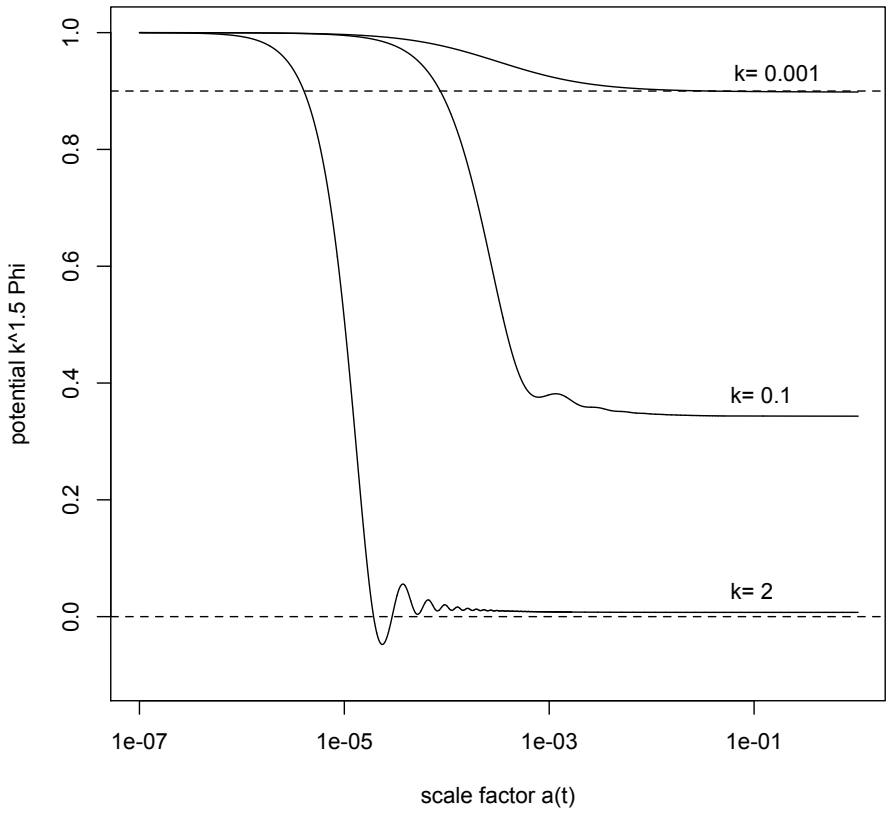

Figure 2.1.: Evolution of the potential Φ for three different perturbation modes k (note that the values given in the figure are in units $h\,\mathrm{Mpc}^{-1}$). Small-scale modes enter the horizon during radiation domination and are damped, i.e. the transfer function is less then unity. In contrast the large-scale modes enter the horizon much later and incur the drop by a factor of 9/10. The effects shown here are due to the transfer function $T(k)$, see below. This agrees with Fig. 7.2 in Dodelson[5].

and see that with constant potential

$$\dot{\delta} = -ikv \qquad \Rightarrow \qquad \ddot{\delta} = -ik\dot{v}. \tag{2.19}$$

Trying the ansatz $\delta = \delta_0\eta^2$ shows that $-ikv = 2\delta_0\eta$ and $-ik\dot{v} = 2\delta_0$. Now we need to check if this satisfies the differential equation for v:

$$-ik(\dot{v} + aHv) = 2\delta_0 - ikv \cdot aH \tag{2.20}$$

$$= 2\delta_0 + 2\delta_0\eta \cdot aH. \tag{2.21}$$

Using the fact that during matter domination $H^2 \propto a^{-3}$ and $a \propto \eta^2$ we see that $aH \propto 1/\sqrt{a} \propto 1/\eta$. This means that the expression in the equation above is indeed constant, and thus satisfies the differential equation (2.6). We thus arrive at the result $\delta \propto a$ for the evolution in matter dominated era. □

Radiation Domination Modes that enter the horizon during radiation domination experience a totally different evolution. In the $\Omega_m = 1$ model we find

$$\Phi(\eta) = \frac{3}{k^2\eta^3}\left(\sin\frac{k\eta}{\sqrt{3}} - \frac{k\eta}{\sqrt{3}}\cos\frac{k\eta}{\sqrt{3}}\right) \cdot \Phi_P \tag{2.22}$$

For a proof consult [5]. This explains the damped oscillations in the potential of small-scale modes in Fig. 2.1.

This analytical expression for the potential Φ can be used to find an expression for the density contrast δ. One finds that

$$\delta(k,\eta) = A\Phi_P \cdot \log(B \cdot k\eta), \qquad A, B \text{ parameters.} \tag{2.23}$$

Once again, a proof can be found in [5]. Hu and Sugiama, [10] find values $A \approx 9.6$ and $B \approx 0.44$ This means that modes, that enter the horizon during radiation domination, i.e. small-scale modes, grow logarithmically during that epoch.

Sub-horizon Evolution

Some time before radiation-matter equality small-scale modes have long entered the horizon: $a \gg a_H$. In Eq. (5.81), however, the radiation perturbation is negligible compared to the $\rho_{\rm dm}\delta$ term and the rest of the equation is suppressed as $aH/k \ll 1$. Again, working with the variable $y := a/a_{\rm eq}$ and defining prime as

differentiation with respect to y one finds the following set of equations:

$$\begin{aligned} \delta' + \frac{ikv}{aHy} &= -3\Phi' \\ v' + \frac{v}{y} &= \frac{ik\Phi}{aHy} \\ k^2\Phi &= \frac{3y}{2(y+1)} a^2 H^2 \delta \end{aligned} \tag{2.24}$$

The solution for δ must adhere to Mezaro's equation for the inhomogeneities:

$$\delta'' + \frac{2+3y}{2y(y+1)}\delta' - \frac{3}{2y(y+1)}\delta = 0. \tag{Mezaro}$$

A proof of the derivation and the following implications of Mezaro's equation is straightforward and can be found in [5]. The solutions to Mezaro's equation are the growth function $D_1(a)$:

$$D_1(y) = y + \frac{2}{3} = \frac{a + 2a_{\mathrm{eq}}/3}{a_{\mathrm{eq}}}, \tag{2.25}$$

and a decaying mode

$$D_2(y) = D_1(y) \log\left(\frac{\sqrt{1+y}+1}{\sqrt{1+y}-1}\right) - 2\sqrt{1+y}. \tag{2.26}$$

Recall that with $a \gg a_H$ we have $y \gg y_H$ and for those modes the general solution to Mezaro's equations is a linear combination between the two:

$$\delta(k,a) = C_1 D_1(y) + C_2 D_2(y), \qquad C_1, C_2 = \text{const.} \tag{2.27}$$

This expression must match onto the logarithmic growth during radiation domination seen in the last section, Eq. (2.23) within the matching domain where the mode has entered the horizon but radiation-matter transition has not happened yet. We will use this technique to derive an expression for the transfer function on small scales below.

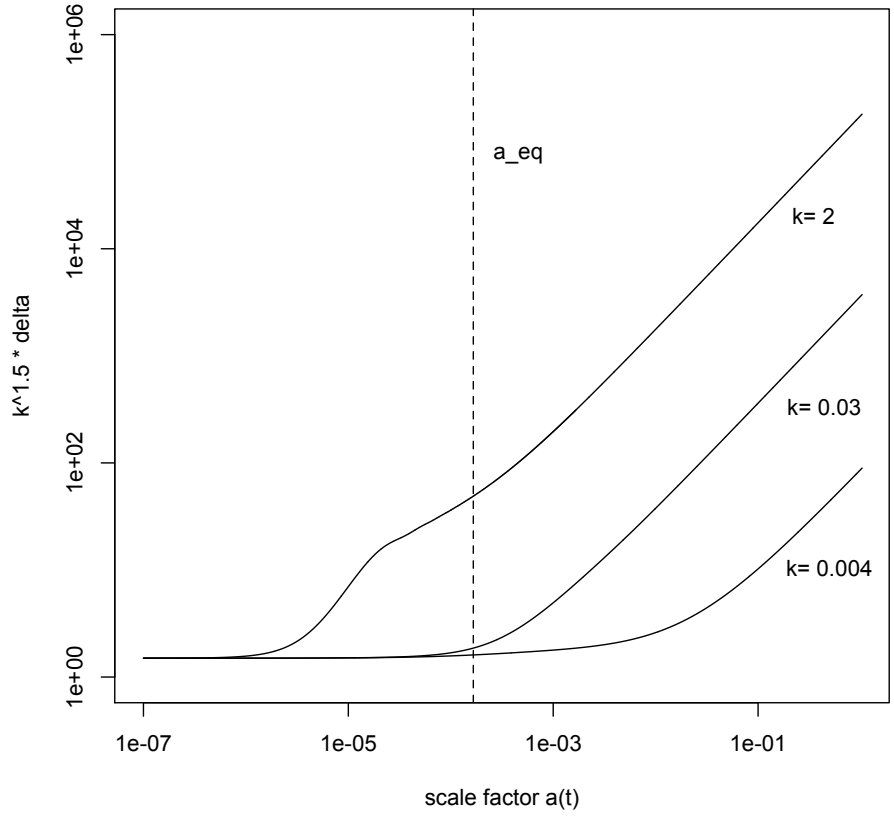

Figure 2.2.: This plot shows the growth of the density perturbations. There is a stark k-dependence of the growth: smaller modes start growing earlier, but are suppressed during radiation domination before and during a_{eq} (which is indicated as vertical dotted line). Bigger modes start later and grow freely in matter domination. At late times all modes grow proportionally to a. Note that k is again given in units of $h\,\mathrm{Mpc}^{-1}$. This agrees with Fig. 7.3 in Dodelson[5].

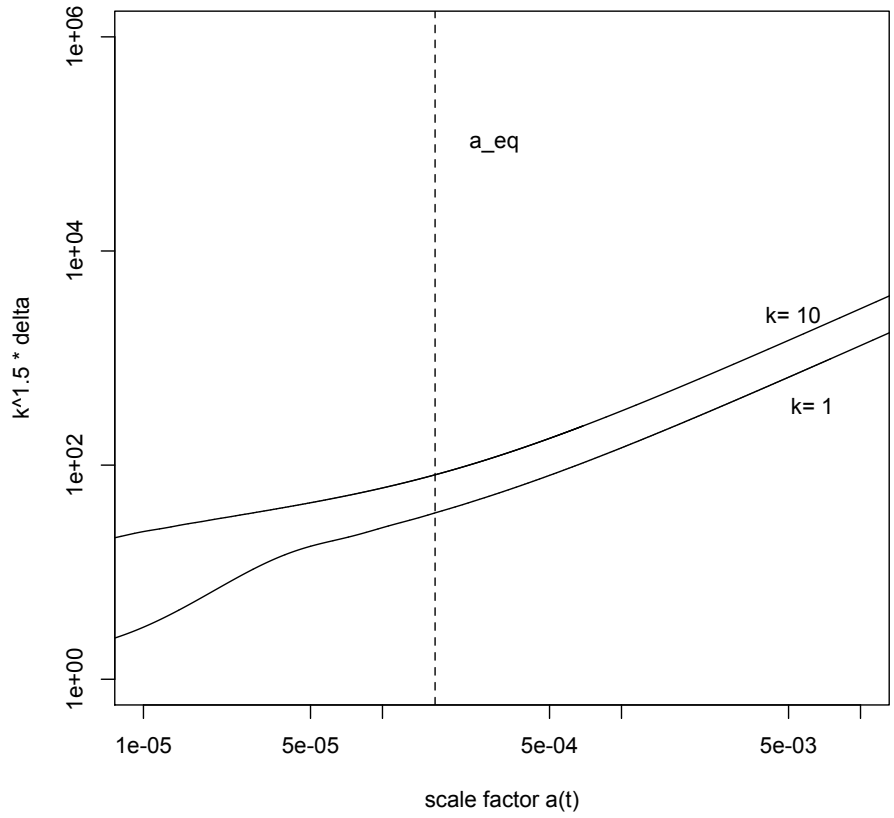

Figure 2.3.: This plot shows the behaviour of the two modes $k = 1$ and $k = 10h\,\mathrm{Mpc}^{-1}$ early in the universe. Mezaro's equation applies to the area left of the a_{eq} line. There the agreement is very good (not shown here).

2.2. Numerical Simulation

The most natural and straightforward thing to do with the set of coupled differential equations of the full Boltzmann-Einstein system, Eq. (2.4) and following, is to put everything on a computer. A sensible result will be to see how the perturbations develop, what happens to the potential Φ and the inhomogeneities δ. Even better, we can hope for a confirmation (as already indicated above) of the analytical work of the last section.

For reasons of completeness we repeat the equations governing the full Boltzmann-Einstein system:

$$\dot{\Theta}_{r,0} + k\Theta_{r,1} = -\dot{\Phi} \tag{2.4}$$

$$\dot{\Theta}_{r,1} + \frac{k}{3}\Theta_{r,0} = \frac{-k}{3}\Phi$$

$$\dot{\delta} + ikv = -3\dot{\Phi} \tag{2.6}$$

$$\dot{v} + \frac{\dot{a}}{a}v = ik\Phi,$$

Additional to that we use the differential expression Eq. (2.8) in the form:

$$\dot{\Phi} = \frac{1}{3\dot{a}}\frac{3H_0^2}{2}(\Omega_m\delta + 4\Omega_r\Theta_{r,0}a^{-1}) - ak^2\Phi - \frac{\dot{a}}{a}\Phi \tag{2.28}$$

Proof. This follows directly from Eq. 2.8 when resolving for $\dot{\Phi}$ and inserting

$$4\pi G\rho_{\mathrm{cr}} = \frac{3}{2}H_0^2. \tag{2.29}$$

□

The parameter of the simulation here are $h = 0.5, \Omega_m = 1$ and $\Omega_r = 10^{-5}$.

The initial conditions are the values for the variables at the end of inflation (the time of the start of this simulation). Inflationary models give the following relations between the potential Φ and the other values:

$$\Theta_{r,0} = \frac{1}{2}\Phi \tag{2.30}$$

$$\Theta_{r,1} = -\frac{a}{6\dot{a}}k\Phi \tag{2.31}$$

$$\delta = 3\Theta_{r,0} \tag{2.32}$$

$$iv = -\frac{1}{2}\frac{k\Phi a}{\dot{a}} \tag{2.33}$$

For the potential itself we insert $\Phi = k^{-3/2}$ in order to normalise the spectrum.

The simulation itself is a numerical integration of the system of coupled equation in the programming language `C++`. There is a wide range of existing numerical integrators readily available, several of which can be found in `Numerical Recipes`[14]. Here we use a Runge-Kutta based integration technique called `Stepperdopr853` from this book. It is a Dormand-Prince embedded method of order eight that uses 12 function evaluations per step. Closely watched by a superordinate instance of the program it ensures adaptive stepsize control at all times of the integration. This ensures that the numerical error is kept to a minimum, the integrator will bulk, as soon as it finds the results not reliable.

In the following we will discuss the physics of the evolution of the inhomogeneities and – as we go along – discuss the numerical methods applied to find these results. All figures – including the figures above and in Chapter 1 – come from this simulation if not otherwise stated.

The additional equation we use is Eq. (5.81). This has the advantage that it minimises the difficulties of a numerical integration. The only problem arises for small scale modes at relatively late times. This is because it becomes tricky to trace the behaviour of the radiation perturbations. However, these modes have long entered the horizon and well after radiation-matter transition radiation becomes negligible. The idea is to halt the integration process at this stage and restart it without following the radiation anymore. There is the caveat left, however, that the gravitational potential Φ still does not completely stabilise. Instead, it rapidly oscillates with a tiny amplitude of about 0.1%. This makes it too difficult to track for the numerical integrator. In order to prevent that we manually insert an exponential damping of $d/d\eta(\Phi) = \dot{\Phi}$ so that Φ stabilises in accordance to Eq. (2.18).

The procedure will thus be as follows: We integrate the full system as far as possible to find the k-dependent bulk times of the integrator. Equipped with this knowledge we will be able to stop the integration process just before that and restart it without the differential equations for the radiation perturbations. Additional to that we insert the damping factor in the differential equation for Φ.

Integration until $\eta_{\texttt{STOP}}$

When attempting to integrate the full Boltzmann-Einstein system until today the integrator will – for some small k – bulk at late times. As the integration is in η, we will have to find that $\eta_{\texttt{STOP}}(k)$ until which we can integrate safely. This

function depends on the numerics of the integrating computer, here we suggest

$$\eta_{\texttt{STOP}}(k) = \eta_{\text{today}} - \frac{2}{3}\log\left(100k/(h\,\text{Mpc}^{-1})\right), \tag{2.34}$$

where we set $\eta_{\texttt{STOP}} = \eta_{\text{today}}$ when the second term becomes negative. This means that $\eta_{\texttt{STOP}} \leq \eta_{\text{today}}$. What this means for the integration is shown in Fig. 2.4. The red line indicates up to where an integration of the full system is done when following Eq. (2.34), i.e. the left side of the red line has been integrated with the full system, the right side with the damped system. The points on the red lines show the k-dependence of the coordinates:

$$(a_{\texttt{STOP}}(k), \Phi(k, a_{\texttt{STOP}}(k))), \tag{2.35}$$

where we define in accordance with Eq. (2.34) that $a_{\texttt{STOP}} := a(\eta_{\texttt{STOP}})$. From this plot we see already that the algorithm only switches to the damped system when Φ has been constant for some time. Fig. 2.5 and 2.6 give more insight into the behaviour of the potential Φ where it crosses the red line (see below).

The Damping Factor

We insert an exponential damping factor $\texttt{damp}(k, \eta)$ into Eq. (2.28) and at the same time dropping the radiation perturbations. The equation then reads

$$\dot{\Phi} = \left[\frac{1}{3\dot{a}}\left(\frac{3}{2}H_0^2\Omega_m\delta - ak^2\Phi\right) - \frac{\dot{a}}{a}\Phi\right] \cdot \texttt{damp}(k, \eta). \tag{2.36}$$

The form of the damping term $\texttt{damp}(k, \eta)$ has to be chosen such that the lines on the left of the red line in Fig. 2.4 match smoothly onto those on the right. The k-dependence stems from the fact that larger modes (small k) do not need to be damped as strongly as smaller modes. In fact modes of wave vector $k \simeq 0.01h\,\text{Mpc}^{-1}$ and larger do not need to be damped at all: It is possible to integrate the full system all the way up to today. In that case we set $\eta_{\texttt{STOP}} = \eta_{\text{today}}$, as mentioned above. This is why the red line in Fig. 2.4 does have a upper limit. In the treatment here we choose for the damping factor:

$$\texttt{damp}(k, \eta) = \eta^{-(1+0.1k)}. \tag{2.37}$$

Fig. 2.5 shows the behaviour of the mode $k = 0.5h\,\text{Mpc}^{-1}$, i.e. the evolution of Φ at times shortly before the integration of the full system will bulk. The black

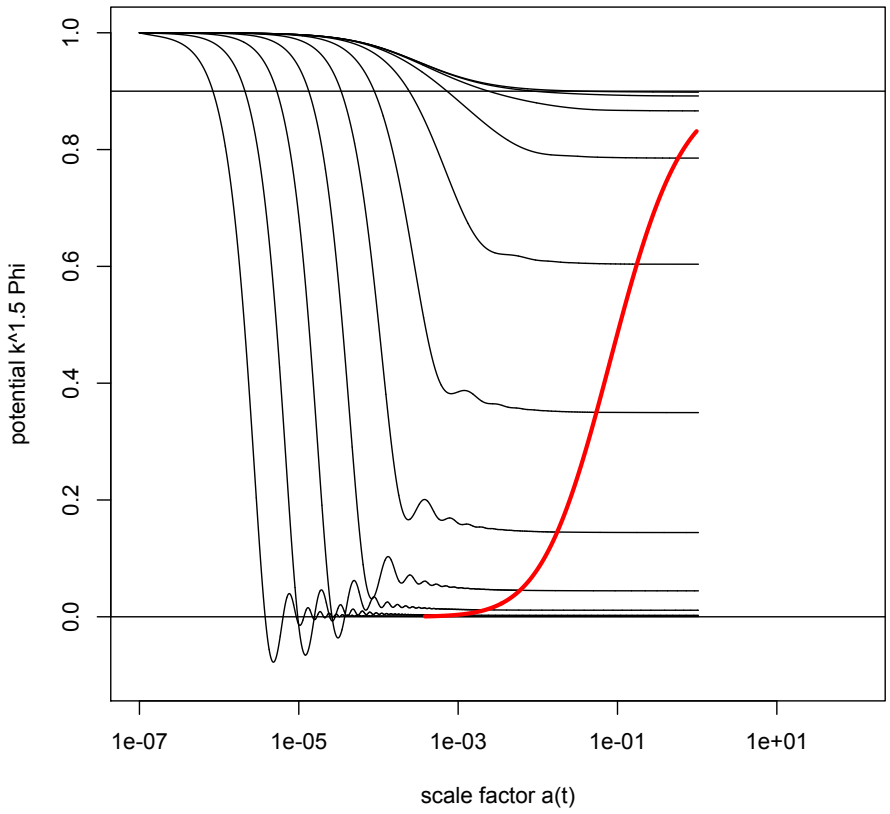

Figure 2.4.: Just as Fig. 2.7 this plot shows the evolution of Φ of 10 modes. Additional to that the red line indicates that the points on the left have been calculated using the full system, whereas the points on the right have been calculated using the damped system. The line has been calculated using Eq. (2.34).

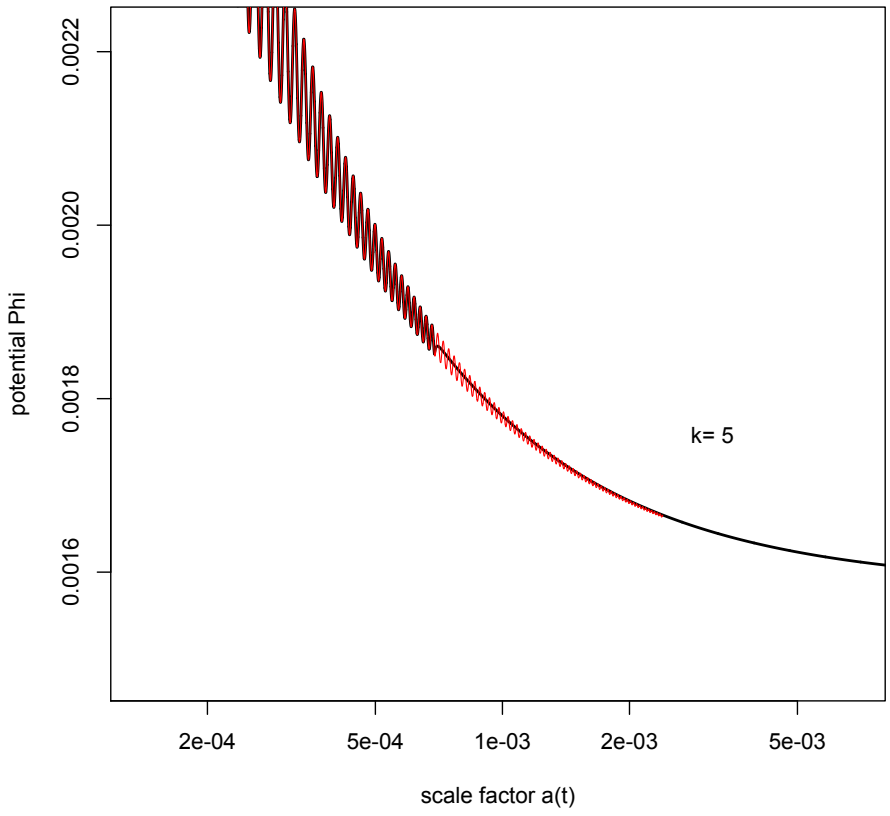

Figure 2.5.: This plot shows in detail the behaviour of the mode with wave vector $k = 5h\,\mathrm{Mpc}^{-1}$. The integration of the full system (integrated as far as possible) is shown in red, the integration of the system that has been stopped and started again with the damping factor is shown in black (and integrated until today).

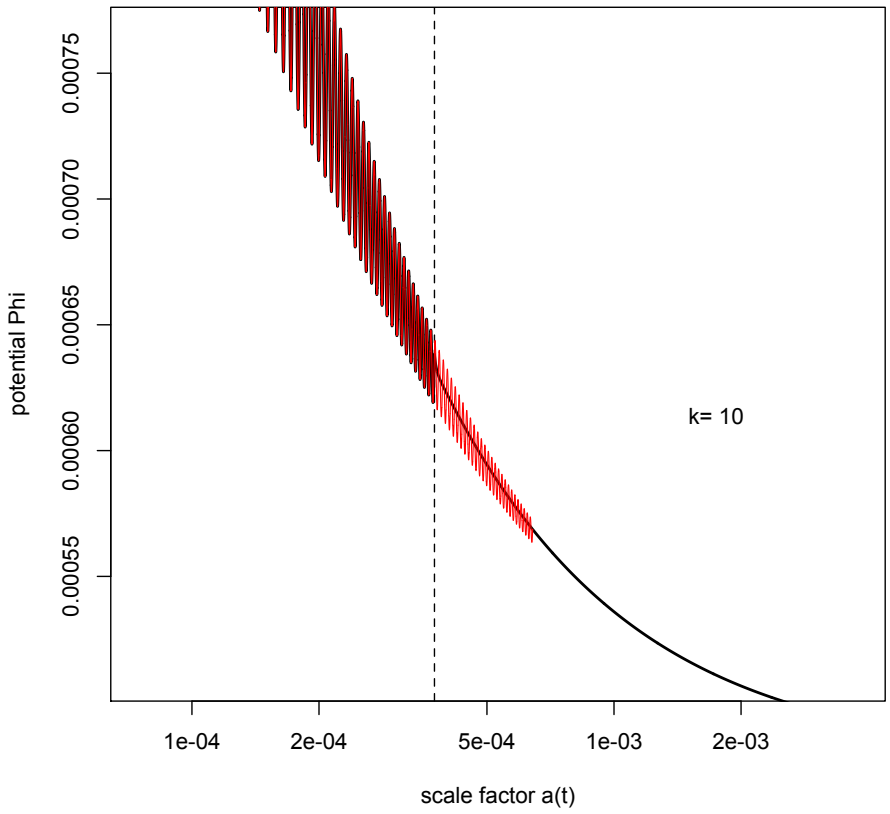

Figure 2.6.: This plot shows the detailed behaviour of the mode $k = 10h\,\mathrm{Mpc}^{-1}$. The colouring follows Fig. 2.5

line shows the evolution of the system with the damping factor with $\eta_{\texttt{STOP}}$ chosen according to Eq. (2.34), the red line that of the full (undamped) system integrated slightly further.

The vertical, dashed line indicates the scale factor at which the simulation with the damping factor has been stopped. This corresponds to the intersection of the red line with the line representing Φ in Fig. 2.4. The oscillations before that are, of course, shared by both curves: Here, the differential equations are exactly the same. After that the black line does not show the oscillations of the full system anymore. This is because they have their origin in the rapidly changing radiation perturbations which are ignored at this stage in the black model. However, the overall behaviour is very well approximated by the damped model, as it traces the full system very accurately.

Fig. 2.6 shows the corresponding plot for the mode $k = 10h\,\mathrm{Mpc}^{-1}$.

2.3. The Evolution of Inhomogeneities

Fig. 2.1 shows the evolution of the potential Φ for different modes. The potential of large-scale modes ($k \sim 0.001\,h\mathrm{Mpc}^{-1}$) is up to a 10% drop unaffected by radiation-matter transition. However, small-scale modes ($k \sim 1\,h\mathrm{Mpc}^{-1}$) suffer a substantial drop.

Analytically we describe the potential at late times a_{late} and thereafter by its primordial value Φ_P, the so called transfer function $T(k)$ and the growth function $D_1(a)$. The normalisation is chosen as

$$\Phi(\mathbf{k}, a) = \frac{9}{10}\,\Phi_P(\mathbf{k})\,T(k)\,\frac{D_1(a)}{a} \qquad \text{for } a > a_{\mathrm{late}}. \tag{2.38}$$

This equation is only valid at late times, i.e. a sufficiently large time interval after radiation-matter transition. We will assume this for the rest of the chapter.

The Transfer Function $T(k)$

The transfer function describes the change of potential $\Phi(\mathbf{k}, a)$ during radiation-matter equality and horizon crossing for the different modes k. The formal definition is given by

$$T(k) := \frac{\Phi(k, a_{\mathrm{late}})}{\Phi_{\text{large-scale}}(k, a_{\mathrm{late}})}. \tag{2.39}$$

The factor of 9/10 in Eq. (2.38) ensures that the transfer function is unity for the largest modes that only today start entering the Hubble horizon (see above for a derivation). But, as we see in Fig. 2.1, this is clearly not the case for smaller modes: There is a substantial drop in potential in these modes compared to the large-scale modes. This is because small modes enter the horizon during radiation domination and causal physics starts to act on them. The earlier they enter the more suppressed they are in accordance with the theoretical results derived above. For those modes we can predict the transfer function to be

$$T(k) \simeq \frac{12k_{\mathrm{eq}}^2}{k^2} \cdot \log\left(\frac{k}{8k_{\mathrm{eq}}}\right) \qquad \text{for } k \gg k_{\mathrm{eq}}. \tag{2.40}$$

Proof. The proof uses the solution to Mezaro's equation we derived earlier:

$$\delta(\mathbf{k}, y) = C_1 D_1(y) + C_2 D_2(y), \tag{2.41}$$

again defining $y = a/a_{\mathrm{eq}}$. As mentioned above this solution can be matched onto

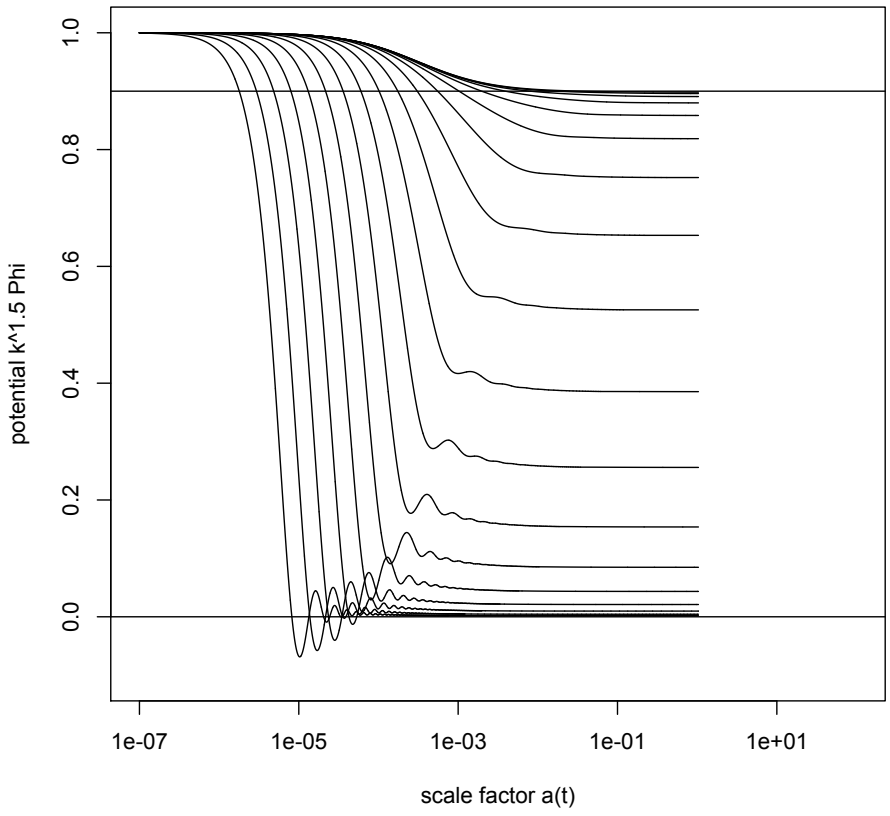

Figure 2.7.: This plot in principle resembles Fig. 2.1: it shows potential Φ versus scale factor a. Here, a scan on different values for k has been performed: The lines shown correspond to $0.001h\,\mathrm{Mpc}^{-1} \cdot 1.64^i$, $i = 0, 1, \ldots, 18$. This plot basically shows the effect of the transfer function on the potential.

the logarithmically growing mode deep in radiation dominated era

$$\delta(k,\eta) = A\Phi_P \log(B\,k\eta). \tag{2.23}$$

Deep in radiation era means that the argument $k\eta$ can be replaced by y/y_H because $k = a_H H(a_H) = a_H\sqrt{H_0^2\Omega_r a^{-4}} \propto 1/a_H$ and $a \propto \eta$. The matching conditions (for the function and its derivative) then become:

$$A\Phi_P \cdot \log(By/y_H) = C_1 D_1(y) + C_2 D_2(y) \tag{2.42}$$

$$A\Phi_P \,\frac{y_H}{By}\,\frac{B}{y_H} = C_1 D_1'(y) + C_2 D_2'(y) \tag{2.43}$$

where y in the matching region. Multiplying the first equation by D_2' and the second by D_2 we can subtract one from another to get rid of the the term proportional to C_2:

$$C_1(D_1 D_2' - D_1' D_2) = A\Phi_P \left[D_2' \,\log\left(\frac{By}{y_H}\right) - \frac{D_2}{y}\right]. \tag{2.44}$$

The term in brackets on the left hand side can be written as $D_1^2\, d/dy(\frac{D_1}{D_2})$ and we use the result from the derivation of the solution of Mezaro's equation to see that this is equal to:

$$D_1^2 \,\frac{d}{dy}\left(\frac{D_1}{D_2}\right) = D_1^2 \frac{-4}{(2+3y)^2}\,\frac{1}{y(\sqrt{1+y})}. \tag{2.45}$$

This means that then

$$D_1 D_2' - D_1' D_2 = \; -\frac{4}{9}\frac{1}{y\sqrt{1+y}} \tag{2.46}$$

$$\simeq \; -\frac{4}{9}\frac{1}{y} \qquad \text{for } y_H \ll y \ll 1. \tag{2.47}$$

In the same limit we approximate

$$D_2(y) \simeq \frac{2}{3}\log(4/y) - 2 \qquad \text{and} \tag{2.48}$$

$$D_2'(y) \simeq \; -\frac{2}{3y} \tag{2.49}$$

Plugging back all these results back into Eq. (2.44) we find:

$$-\frac{4}{9y}C_1 \simeq A\Phi_P \left[-\frac{2}{3y}\log(By/y_H) - \frac{1}{y}\left(\frac{2}{3}\log(4/y) - 2\right)\right] \tag{2.50}$$

$$\Rightarrow \quad C_1 \simeq \frac{3}{2} A\Phi_P \left(\log(4B/y_H) - 3\right) \tag{2.51}$$

Having fixed the constant C_1 we see that we do not need to find the value for C_2, because well after equality the decaying mode has long died out. Thus we arrive at a final expression for δ:

$$\delta(\mathbf{k}, a) = \frac{3}{2} A\Phi_P(\mathbf{k}) \left(\log(4B/y_H) - 3\right) D_1(a). \tag{2.52}$$

To turn this into a result for the transfer function we use the relation between δ and Φ_P from below, Eq. (7.8)

$$\delta(\mathbf{k}, a) = \frac{3}{5} \frac{k^2}{\Omega_m H_0^2} \Phi_P(\mathbf{k})\, T(k) D_1(a). \tag{7.8}$$

Equating the two expressions for δ, dropping the terms D_1 and Φ_P and resolving the resulting equation for the transfer function $T(k)$ we see – using $a_{\rm eq}/a_H = \sqrt{2}k/k_{\rm eq}$ – that

$$T(k) = \frac{5}{2} A \frac{\Omega_m H_0^2}{k^2 a_{\rm eq}} \cdot \log\left(\frac{4Be^{-3}\sqrt{2}k}{k_{\rm eq}}\right) \quad \text{for } k \gg k_{\rm eq}. \tag{2.53}$$

Lastly, we use the definition of $k_{\rm eq} = a_{\rm eq} H(a_{\rm eq}) = \sqrt{2} H_0 a_{\rm eq}^{-1/2}$ with $\Omega_m = 1$ to see that the numerical factors of the transfer function only depend on the ratio $k/k_{\rm eq}$. Recalling the numbers $A = 9.6$ and $B = 0.44$, we see that the numerical factor in the transfer function are 12.0 and $0.124 \simeq 1/8.07$. This finishes the proof of Eq. (2.40). □

The BBKS Fitting Function

Bardeen, Bond, Kaiser and Szalay, [2], have found a fitting function to the transfer function $T(k)$. They define $x := k/k_{\rm eq}$, then

$$T(x) = \frac{\log(1 + 0.171x)}{0.171x} \left(1 + 0.284x + (1.18x)^2 + (0.399x)^3 + (0.490)^4\right)^{-1/4} \tag{2.54}$$

Fig. 2.8 shows the transfer function for the modes relevant in cosmology.

The Growth Function $D_1(a)$

The growth function describes the evolution of the inhomogeneities at late times. In contrast to the transfer function $T(k)$ it is independent of k. Although the

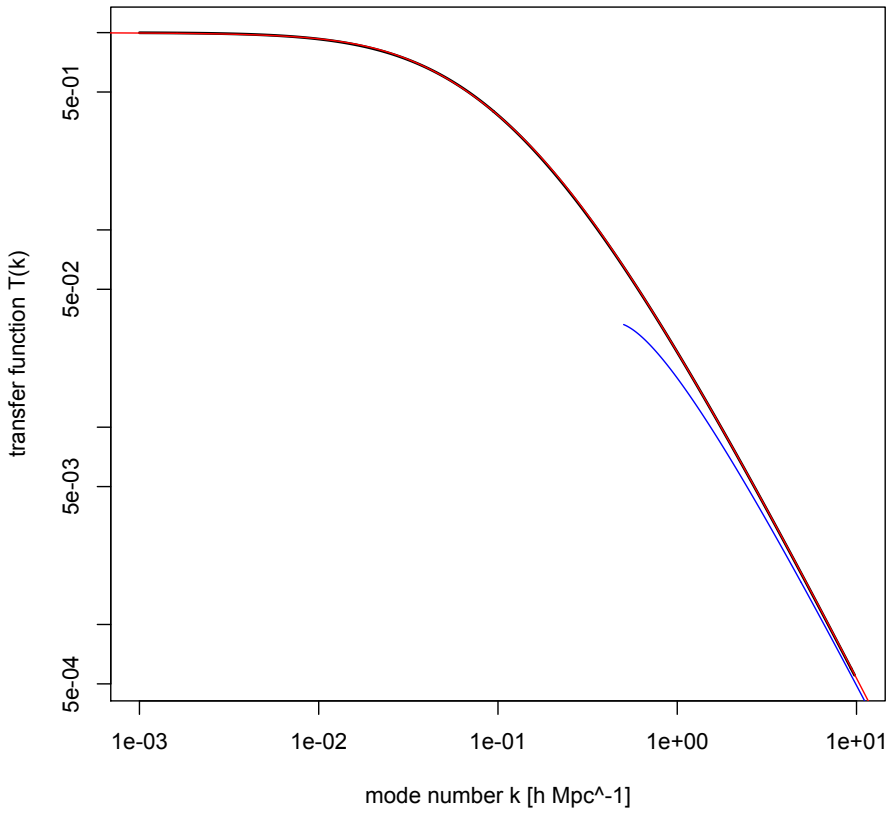

Figure 2.8.: This is a double logarithmic plot of the transfer function versus mode number k: black line (values from the simulation), red line (the BBKS fitting form, [2]) and the blue line (the analytic expression, Eq. (2.40)). On large scales the transfer function is close to unity. On small scale it falls off rapidly following the analytic expression.

potential is constant at late times, matter overdensities have acquired considerable mass already and hence attract more matter. Their growth is exemplary shown in Fig. 2.2 for three different modes, where we explicitly see that their late evolution is mode-independent: they grow as $\delta \propto a$.

The large-scale mode only entered the horizon at late times during matter domination. It starts growing without obstruction. The small-scale mode entered the horizon well in radiation domination. Its suppression from the transfer function (i.e. radiation pressure) can be seen clearly.

At later times well after radiation-matter transition the evolution is determined by the growth factor only and it is the same as for the other modes. The kind of suppression will be an important tool in the determination of the parameter of our universe.

As we have seen already, the growth factor D_1 in a flat matter-dominated universe ($\Omega_m = 1$) is given by:

$$D_1(a) = \frac{a}{a_{\mathrm{eq}}} - \frac{2}{3}. \tag{2.55}$$

Defining $x := (1 - \Omega_m)a/\Omega_m$ the growth factor in an open matter-dominated universe ($\Omega_m < 1$) is given by

$$D_1(a) = \frac{5\Omega_m}{2(1-\Omega_m)} \left[3\frac{\sqrt{1+x}}{x^{3/2}} \log\left(\sqrt{1+x} - \sqrt{x}\right) + 1 + \frac{3}{x} \right] \tag{2.56}$$

Proof. A proof of this formula will be given in the next Chapter, on page 56. This is because we will need the general Friedmann equation (here for matter and curvature) and its consequences on the growth function. This is being discussed in the chapter on dark energy and its consequences on the evolution of matter inhomogeneities. □

Fig. 2.9 shows the growth factor for four different models of the universe for $a = 0.1$ to $a = 1$. The top line corresponds to the flat, matter dominated universe, the three lines below that to open, matter dominated universes with varying Ω_m. The growth factor in the flat case, Eq. (2.55) coincides with the ($\Omega_m \to 1$)-limit of Eq. (2.56) as well as with the data from the simulation. This is a very important consistency check.

We see from these curves that the growth factor $D_1(a)$ behaves almost identically up to $a \sim 0.1$. In the flat case the growth factor is simply proportional to the scale factor, see Eq. (2.55). In the open models the growth factor is increasingly suppressed with decreasing matter content. The structures we see today must

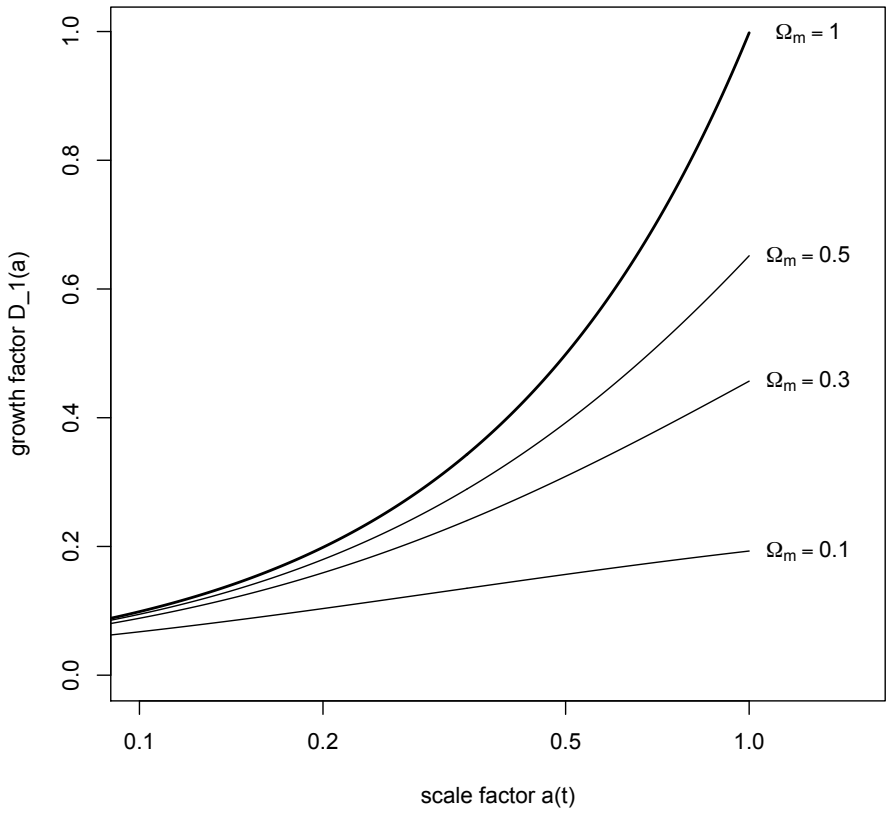

Figure 2.9.: Here the growth factor is shown for a flat, matter dominated ($\Omega_m = 1$) universe and several open, matter dominated ($\Omega_m < 1$) universes. The growth factor in the flat case (thick line) is given by Eq. (2.55), in the open case (thin lines below) by Eq. 2.56. The figure has been normalised to the growth factor in the flat case today.

have formed earlier in an open universe compared to a flat, matter dominated universe. Refer to page 58 for a discussion of the effects of dark energy on the growth factor.

2.4. The Matter Power Spectrum

With the machinery developed so far we can explain the power spectrum of the matter distribution at late times. This is important and very helpful for the further discussion, because the power spectrum is accessible to observations via large galaxy redshift surveys. The power spectra of matter $P_\delta(k)$ and gravitational potential $P_\Phi(k)$ are defined via:

$$\langle \delta(\mathbf{k}, a)\delta(\mathbf{k}', a)\rangle = (2\pi)^3 P_\delta(k)\, \delta^{(3)}(\mathbf{k} - \mathbf{k}') \quad \text{and} \tag{2.57}$$

$$\langle \Phi(\mathbf{k})\Phi(\mathbf{k}')\rangle = (2\pi)^3 P_\Phi(k)\, \delta^{(3)}(\mathbf{k} - \mathbf{k}'), \tag{2.58}$$

where the $\delta^{(3)}$ denotes the Dirac delta function in three dimensions.

Scale-free Spectra

A scale-free spectrum $P(k)$ (or scale-invariant) is a spectrum for which the excess power is constant, i. e. independent of k. The (integrated) excess power Δ is defined by

$$\Delta^2(k) := \frac{k^3 P(k)}{2\pi^2}. \tag{2.59}$$

The name comes from the identification of $P(k)d^3k/(2\pi)^3$ with the excess power in the canal centred at at k with width dk. The integration goes over all directions of $\mathbf{k}$. The significance of the excess power is that it is an indicator of nonlinearities in the perturbations. Small inhomogeneities, that can be treated with linear perturbation theory, have small Δ, whereas nonlinear perturbations have a corresponding large excess power Δ. The critical value for the excess power Δ is about 1.

In the case of scalar perturbations (in which we are working here) the potential power spectrum at primordial times is given by

$$P_\Phi(k) = \frac{50\pi^2}{9k^3} \left(\frac{k}{H_0}\right)^{n-1} \delta_H^2 \left(\frac{\Omega_m}{D_1(a=1)}\right)^2. \tag{6.100}$$

This definition (and the equation numbering) follows the conventions of [5]. Note that this idea of the primordial power spectrum includes the growth function D_1 evaluated today at $a = 1$ and the value of the overdensities at horizon crossing δ_H. The number n is an index of the scale invariance of the spectrum. The scale-free spectrum (Harrison-Zel'dovich-Peebles) spectrum corresponds to $n = 1$. The theory of inflation suggests that the scalar (and tensor) perturbations in the universe are scale-free up to small deviations. It is these deviations we are most

interested in, i.e. we are looking for n.

Today's Matter Power Spectrum

To find an expression for today's matter power spectrum we use Eq. (6.100) for the primordial power spectrum and the definition of transfer and growth functions. We find (again with the equation numbering of [5]):

$$P(k,a) = 2\pi^2 \delta_H^2 \frac{k^n}{H_0^{n+3}} T^2(k) \left(\frac{D_1(a)}{D_1(a=1)} \right). \tag{7.9}$$

Proof. At late times the algebraic expression for the gravitational potential $k^2\Phi(\mathbf{k})$ simplifies to

$$k^2\Phi(\mathbf{k}) = 4\pi G a^2 \cdot \rho_m \delta(\mathbf{k}, a). \tag{2.60}$$

This can be seen as follows: Eq. (5.81) in [5] reads:

$$k^2\Phi = 4\pi G a^2 \left[\rho_m \delta_m + 4\rho_r \Theta_{r,0} + \frac{3aH}{k} \left(i\rho_m v_m + 4\rho_r \Theta_{r,1} \right) \right]. \tag{5.81}$$

We now consider the limit of Eq. (5.81) in the case of negligible radiation for large-scale modes. This means that we set $\rho_r = 0$ and take $aH/k \ll 1$ and immediately recover Eq. (2.60).

Upon insertion of $\rho_m/\rho_{\rm cr} = \Omega_m a^{-3}$ (matter domination) and the definition of $\rho_{\rm cr}$ one finds that

$$\begin{aligned} \delta(\mathbf{k}, a) &= \frac{2}{3} \frac{a}{\Omega_m H_0^2} \, k^2 \Phi(\mathbf{k}) \\ &= \frac{3}{5} \frac{k^2}{\Omega_m H_0^2} \Phi_P(\mathbf{k}) \, T(k) D_1(a), \end{aligned} \tag{7.8}$$

where in the second line the analytical expression for $\Phi(\mathbf{k})$, Eq. (2.38), has been inserted (the equation numbering follows [5]). Using the definition of the power spectrum, Eq. (2.57), we find the equation

$$(2\pi)^3 P_\delta(k) \delta^{(3)}(\mathbf{k} - \mathbf{k}') = \langle \delta(\mathbf{k}, a) \delta(\mathbf{k}', a) \rangle \tag{2.61}$$

$$= \frac{9}{25} \frac{1}{\Omega_m^2 H_0^4} \langle k^4 \Phi_P^2 T^2(k) D_1^2(a) \rangle. \tag{2.62}$$

Here, the brackets on the right hand side collapse onto $\langle \Phi_P^2(k) \rangle$ and we can use its definition, Eq. (2.58), to replace it with the potential power spectrum P_Φ. This, in turn, can be replaced by expression (6.100). Dropping the $(2\pi)^3 \delta^{(3)}(\mathbf{k} - \mathbf{k}')$

terms on both sides we see that

$$P_\delta(k,a) = \frac{9}{25}\frac{1}{\Omega_m^2 H_0^4} k^4 T^2(k) D_1^2(a) \cdot \frac{50\pi^2}{9k^3} \left(\frac{k}{H_0}\right)^{n-1} \delta_H^2 \left(\frac{\Omega_m}{D_1(a=1)}\right)^2$$
$$= 2\pi^2 \delta_H^2 \frac{k^n}{H_0^{n+3}} T^2(k) \left(\frac{D_1(a)}{D_1(a=1)}\right), \tag{2.63}$$

where the last line simply follows from evaluating the terms in the line above. □

Fig. 2.10 shows the power spectrum obtained from the simulation. The model shown is a flat, matter dominated model ($\Omega_m = 1$ and $h = 0.5$), called a standard cold dark matter power spectrum, or short sCDM power spectrum. We use Eq. (2.63) to translate the results of the evolution of different modes into a power spectrum. We have two analytical results:

On large scales $P(k) \propto k$.

Proof. This follows directly from Eq. (2.63) when we insert a simple (and approximately correct) inflationary model with $n = 1$ (scale-free spectrum). The transfer function is equal to one for these modes and the growth factor D_1 is mode-independent. □

On small scales the power spectrum is a decreasing function of k.

Proof. We have already seen that the transfer function is a decreasing function of mode number k. This can be seen, for example, in Fig. 2.8. With Eq. (2.63) this translates to a decreasing power spectrum on small scales, because the term in the power spectrum without the transfer function grows only as k^n, whereas the transfer function behaves as $\log(k)/k^2$. □

Because these behaviours must fit together smoothly, we can deduce that there must be a point of turnover in the power spectrum. The physical picture of this is as follows: Large-scale modes do not enter the horizon until late in the universe. Their transfer function is thus unity. By the time of horizon entering radiation is negligible and the inhomogeneities grow without impediment. This means that the signature of inflation imprinted on the power spectrum early in the universe ($P \propto k$) is preserved throughout the evolution with time. We see this behaviour on the left hand of the turnover point in Fig. 2.10.

Small-scale modes, however, behave completely different. They enter the horizon early during radiation domination or radiation-matter transition. Causal physics starts to act on them and radiation pressure suppresses their growth, i.e. the transfer function is small and decreasing with k. This can be seen in

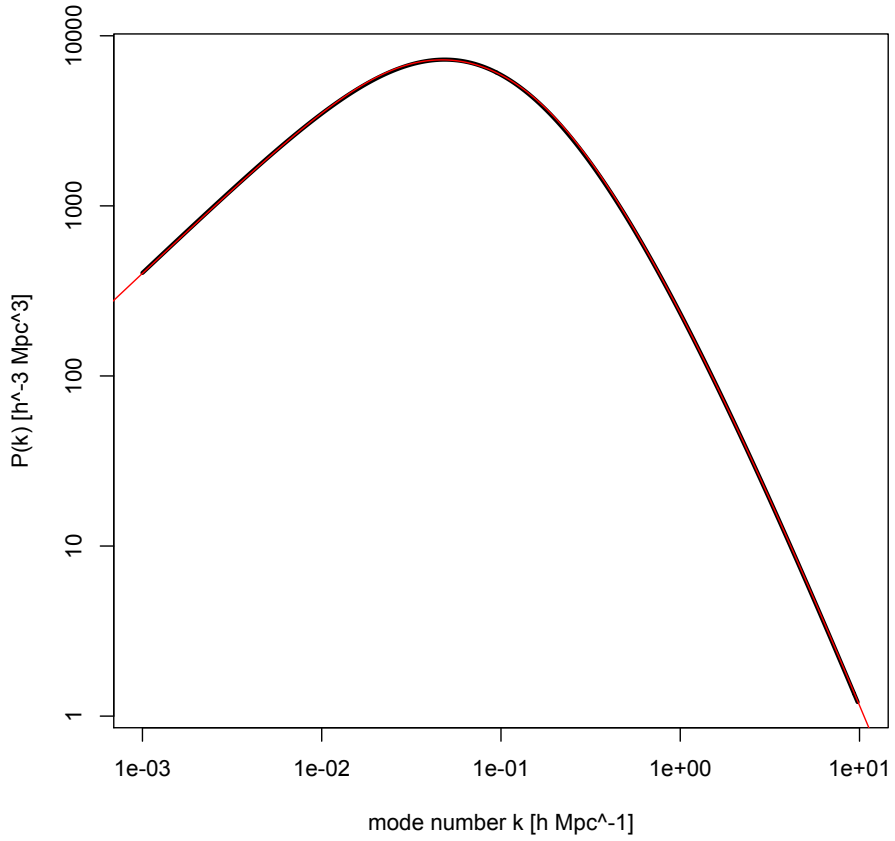

Figure 2.10.: The power spectrum of the inhomogeneities $P_\delta(k)$ today in a $\Omega_m = 1$ model of the universe: sCDM power spectrum. There is a good agreement between the data from the simulation (black line) and the BBKS fitting function (red line). The overall normalisation has been chosen arbitrarily. For large-scale modes the power spectrum behaves as $P \propto k$, for small-scale modes, in contrast, it falls off with k.

Fig. 2.2: Large-scale modes enter late and simply grow with a, small-scale modes ($k = 2h\,\mathrm{Mpc}^{-1}$ shown there) enter early and experience a phase of delayed growth before radiation becomes negligible. The earlier a mode enters the horizon, the more its growth is suppressed. This results in the power spectrum being a decreasing function of k.

In the next chapter we will supplement this discussion with the power spectrum of a model of the universe with cosmological constant Λ. For further discussions [16] and [11] are good starting points.

3. The Effect of Dark Energy on the Inhomogeneities

In the last chapter we extensively discussed the evolution of matter perturbations in a universe with radiation and (dark) matter only. This was very advantageous in the sense that we were able to understand the reasons behind certain features in the evolution of the inhomogeneities. In particular we have seen that the inhomogeneities grow immensely in a matter dominated era of the universe. We did not have to worry about effects of dark energy. In this chapter, however, we set off to discuss the changes caused by dark energy in the universe. We will limit ourselves to dark energy implemented as a cosmological constant Λ in this chapter, and defer all effects due to variable dark energy to the next chapter.

The effect of dark energy is very prominent in both the transfer function $T(k)$ and the growth function $D_1(a)$. Due to their input to the power spectrum we can expect prominent dark energy features in the power spectrum as well. In fact, because of observations of the matter power spectrum in the last 20 years, these effects can be used to find the parameters of the universe we live in.

In the following we compare the results of a simulation of the model with parameter $\Omega_r = 4.67{\cdot}10^{-}5/h^2, \Omega_m = 1$ and $h = 0.5$ on the one hand and the model with cosmological constant with parameters $\Omega_r = 4.67 \cdot 10^{-5}, \Omega_m = 0.3, \Omega_\Lambda = 0.7$ and $h = 0.73$ on the other hand.

3.1. The Transfer Function in a Universe with Λ

The transfer function in models of the universe with Λ behaves differently at late times. This is due to the decay of the gravitational potential at late times. As an example we show the behaviour of the mode $k = 0.001^h\,\mathrm{Mpc}^{-1}$ in Fig. 3.1. Just as in Fig. 2.1 the mode has constant potential Φ early in the universe. During radiation-matter transition the modes suffers from the 9/10-drop and approaches a constant value again. Only at late times the effects of Λ become prominent and the potential drops substantially. This behaviour is exemplary, the other modes incur a similar drop at late times.

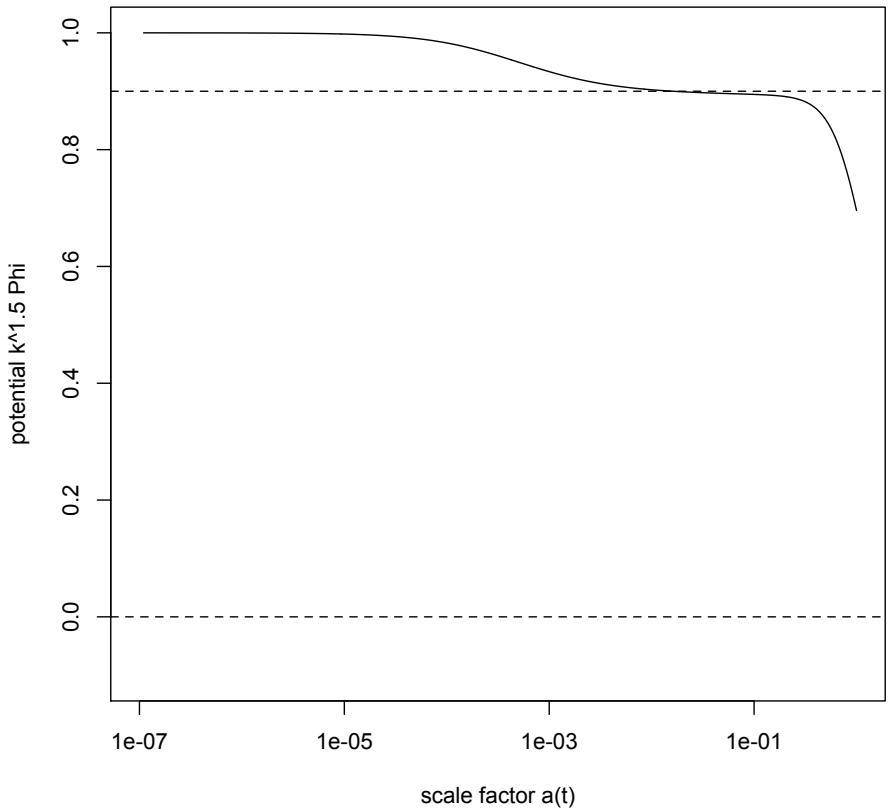

Figure 3.1.: Here we show the decay of the mode $k = 0.001h\,\mathrm{Mpc}^{-1}$ at late times. Even though it is a large-scale mode the gravitational potential suffers from a substantial drop at late times. This is due to the accelerated expansion from the cosmological constant Λ.

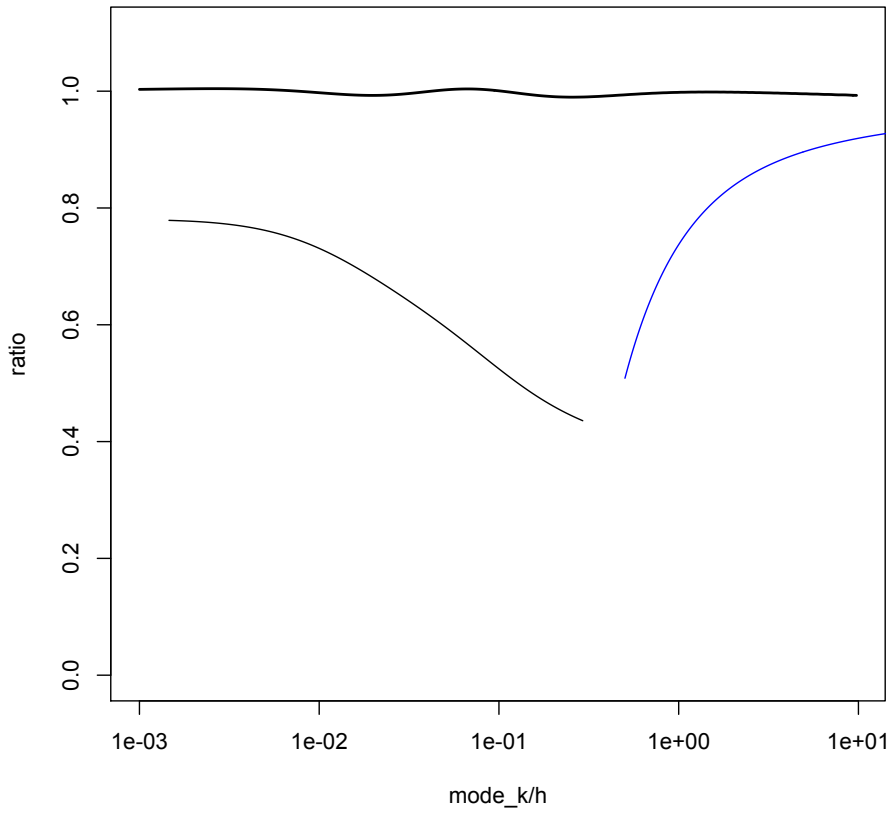

Figure 3.2.: This plot shows the ratio of the transfer function divided by the BBKS fitting form of the transfer function for the model with $\Omega_m = 1$ and $h = 0.5$ (thick black line), the model with Ω_Λ and $h = 0.73$ (thin black line) and the analytic expression, Eq. (2.40) (blue line), c.f. Fig. 2.8 on page 42.

This drop, of course, has radical consequences on the transfer function. Fig. 3.2 shows the transfer function divided by the BBKS form of the transfer function. The thick black line close to unity is the transfer function of the model with $\Omega_m = 1$. From Fig. 2.8 we expect this agreement. The analytic solution, Eq. (2.40) is shown in blue again. As expected, the thin black line of the transfer function of a model with Λ lies substantially below unity.

3.2. The Growth Function in a Universe with Λ

In a flat matter-dominated universe the growth function D_1 was simply given by

$$D_1(a) = \frac{a}{a_{\mathrm{eq}}} - \frac{2}{3}. \tag{3.1}$$

For our universe we suppose this is true for the time after radiation-matter transition, but before the effects of dark energy become apparent, i.e. before $a \simeq 0.1$ or, equivalently, $z \simeq 10$. Even in an open matter-dominated universe we were able to find an analytic expression for the growth function. With dark energy the growth function is given by the integral:

$$D_1(a) = \frac{5\Omega_m}{2} \frac{H(a)}{H_0} \int_0^a \frac{da'}{(a'H(a')/H_0)^3}. \tag{7.77}$$

The advantage of writing it in this form is that it is general enough to include effects of curvature ($\Omega_k \neq 0$). This is important as we are going to use this result to prove Eq. (2.56) from above.

Proof. This proof follows the steps sketched out in [5]. First, we will find the differential equations governing the Boltzmann-Einstein system at late times: $a > 0.1$. Radiation can be ignored (as above), but curvature and dark energy have to be taken into account. This means we attempt to find a generalisation of the Mezaro's equation. For this we retrace the steps of its derivation starting with the system (2.24). The first two equations are valid in this regime, too. However, the derivation of the third equation from the full Boltzmann-Einstein system is not valid anymore. We know that the dark matter behaves like

$$\frac{8\pi G}{3}\rho_{\mathrm{dm}} = H_0^2 \Omega_m a^{-3}. \tag{3.2}$$

This means that the coefficient of the $k^2\Phi$ equation, Eq. (5.81) changes. Again,

we ignore radiation, and deal with modes inside the horizon, so we get:

$$k^2\Phi = 4\pi G a^2 \rho_{\rm dm}\delta = \frac{3}{2}H_0^2\Omega_m a^{-1}\delta. \tag{3.3}$$

Another way to see this is to work with the variable $y := a/a_{\rm eq}$ again. Here we have $y \gg 1$ so that we can approximate $y/(y+1) \approx 1$. This equation together with

$$\begin{aligned} \delta' + \frac{ikv}{aHy} &= -3\Phi' \\ v' + \frac{v}{y} &= \frac{ik\Phi}{aHy} \end{aligned} \tag{2.24}$$

defines the new system of coupled differential equations.

In the derivation of Mezaro's equation we used an expression for the derivative of $1/(aHy)$ with respect to y, but here we want to keep the behaviour of H' as general as possible. This means we will not specify $d/dy(H) = H'$. Similar to the derivation of the Mezaro's equation, we differentiate the differential equation for δ in the system 2.24 to obtain a second-oder equation for δ. The differential equations of the system can be combined to find a second order differential equation for δ, Eq. (7.73):

$$\frac{d^2\delta}{da^2} + \left(\frac{d\log H}{da} + \frac{3}{a}\right)\frac{d\delta}{da} - \frac{3\Omega_m H_0^2\delta}{2H^2a^5} = 0, \tag{7.73}$$

where all factors of $a_{\rm eq}$ disappear.

Interestingly, in several cases there are non-increasing solutions for δ. These are, however, useless for the theory of structure formation. It drops out that the increasing solution in case of matter, cosmological constant and curvature is determined by the integral:

$$I(a) := \int^a \frac{da'}{(a'H(a')/H_0)^3} \tag{3.4}$$

and the coefficients turn out to be the ones given in Eq. (7.77). Note however, that this is no longer true if dark energy has an equation of state with parameter $w \neq -1$, see the discussion on page 64. □

We are now in a position to proof Eq. (2.56), i.e. we want to show that

$$D_1(a) = \frac{5\Omega_m}{2(1-\Omega_m)}\left[3\frac{\sqrt{1+x}}{x^{3/2}}\log\left(\sqrt{1+x}-\sqrt{x}\right) + 1 + \frac{3}{x}\right] \tag{2.56}$$

Proof. To begin with we define a new variable $y := \Omega_m/a$ with

$$dy = -\Omega_m \frac{da}{a^2} \tag{3.5}$$

. Using this variable and the Friedmann equation for an open universe,

$$H^2(a) = H_0^2(\Omega_m a^{-3} + \Omega_k a^{-2}), \quad \text{where } \Omega_k = 1 - \Omega_m, \tag{3.6}$$

$$= \frac{H_0^2}{a^2}(y + 1 - \Omega_m) = \frac{H_0^2}{\Omega_m^2} y^2 (y + 1 - \Omega_m) \tag{3.7}$$

$$\Rightarrow \frac{H_0^3}{aH^3(a)} = \frac{a^2}{(y + 1 - \Omega_m)^{3/2}} = \frac{\Omega_m^2}{y^2} \frac{1}{(y + 1 - \Omega_m)^{3/2}} \tag{3.8}$$

we see that the integral $I(a)$ of Eq. (3.4) and Eq. (7.77) transforms as

$$\Omega_m \int_0^a \frac{da'}{(aH(a)/H_0)^3} = \int_{\Omega_m/a}^{\infty} \frac{\Omega_m^2 \, dy}{y^2 (y + 1 - \Omega_m)^{3/2}} \tag{3.9}$$

We now use a common trick in solving integrals: We introduce new variables ϵ and λ realising that the product of

$$\frac{d}{d\epsilon} \frac{1}{y + \epsilon}\bigg|_{\epsilon=0} = \frac{-1}{y^2} \qquad \text{and} \tag{3.10}$$

$$\frac{d}{d\lambda} \frac{1}{\sqrt{y + \lambda}}\bigg|_{\lambda=1-\Omega_m} = \frac{-1}{2\sqrt{y + 1 - \Omega_m}} \tag{3.11}$$

gives the integrand on the right hand side of Eq. (3.9). All functions are sufficiently smooth, so we can pull the differentiations in front of the integral. The integral then takes the following form:

$$\Omega_m \int_0^a \frac{da'}{(aH(a)/H_0)^3} = 2\Omega_m^2 \frac{d}{d\epsilon} \frac{d}{d\lambda} \int_{\Omega_m/a}^{\infty} \frac{dy}{(y + \epsilon)\sqrt{y + \lambda}}\bigg|_{\substack{\epsilon=0 \\ \lambda=1-\Omega_m}} \tag{3.12}$$

The resulting integral can be done using entry 2.246 in Gradshteyn and Ryzhik, [8], which is for convenience repeated in the Appendix as Eq. (A.1) on page 66 of this document. The expression obtained this way needs to be differentiated with respect to both, ϵ and λ, and then evaluated at $\epsilon = 0$ and $\lambda = 1 - \Omega_m$. That the result is indeed Eq. (2.56) is demonstrated by calculation. □

Equipped with Eq. (7.77) we are now in a position to investigate the growth factor in a variety of universes. This will generalise the discussion of the growth factor in an open, matter dominated universe, see Fig. 2.9 on page 44. Fig. 3.3 shows the growth factor for three different models. We already now the purely

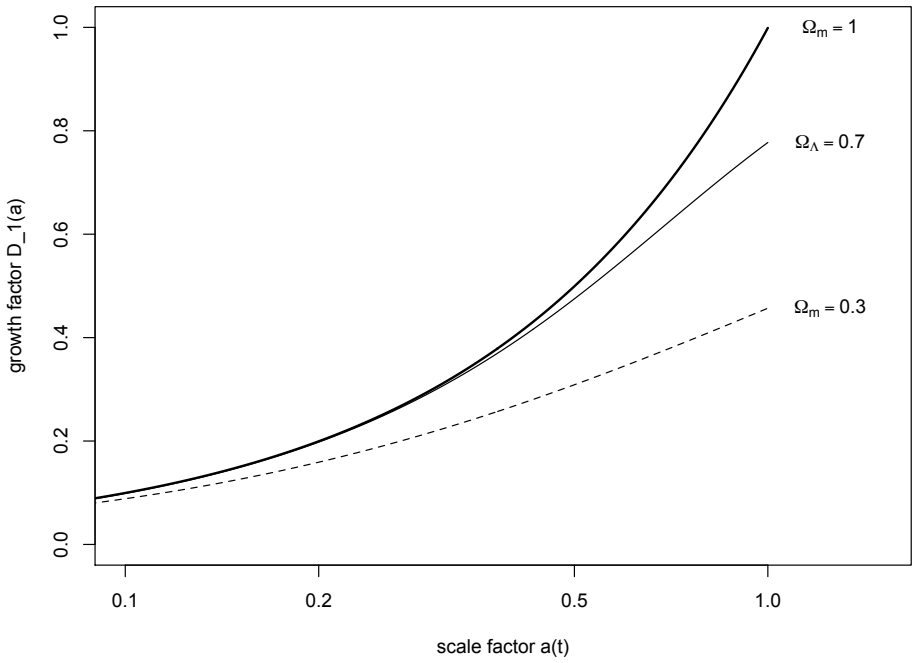

Figure 3.3.: This plot shows the growth factor for three different models for the universe. The two upper curves correspond to flat cas with parameters $(\Omega_m = 1, \Omega_\Lambda = 0)$ and $(\Omega_m = 0.3, \Omega_\Lambda = 0.7)$. The lower curve is the growth factor in an open, matter dominated universe. This agrees with Fig. 7.12 in [5].

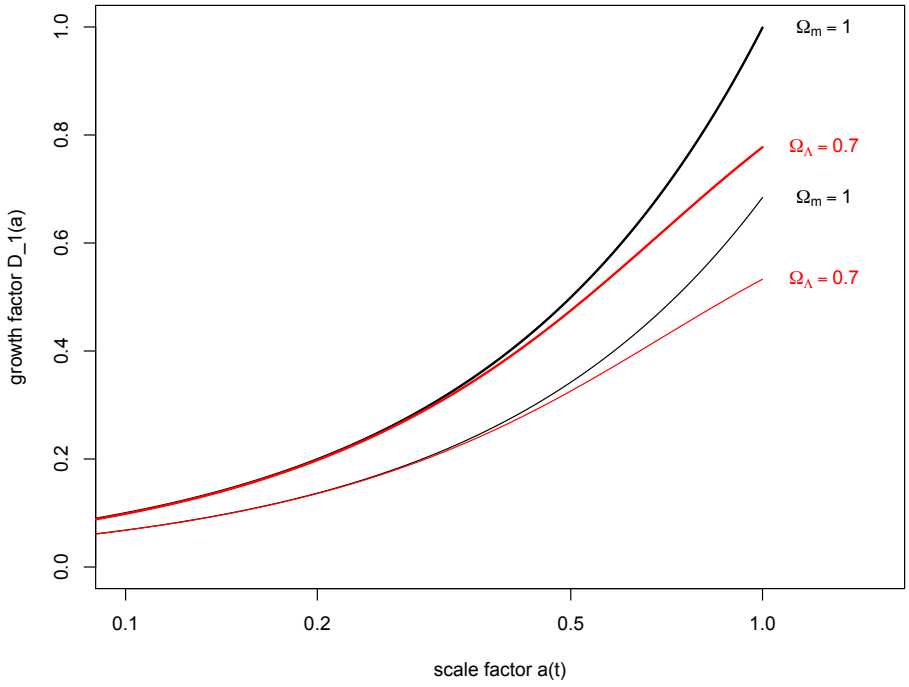

Figure 3.4.: Here the growth factor is shown for four flat models of the universe: The two upper curves have $h = 0.5$, the two lower curves, however, have $h = 0.73$. The black lines correspond to models without Λ ($\Omega_m = 1$), the red lines to universes with Λ ($\Omega_m = 0.3, \Omega_\Lambda = 0.7$).

matter dominated cases (top and bottom curves). The curve in between is the growth factor of a flat universe with matter and Λ, here ($\Omega_m = 0.3, \Omega_\Lambda = 0.7$). When dark energy has not come into effect yet ($a \sim 0.1$ to 0.5), the growth factor of the universes with and without Λ behaves very similarly. Later in time, however, the growth factor in the model with Λ is suppressed compared to the purely matter dominated case. Recalling the fact that the growth factor describes the growth of inhomogeneities at late times we see that in the matter dominated case structures keep building up until today. In the model with Λ, however, the structures we observe today must have formed much earlier as their growth is suppressed at very late times.

Fig. 3.4 shows the two flat models again, this time, however, compared to two corresponding lines with different h. The two upper curves are from models with $h = 0.5$, the two lower ones from curves with $h = 0.73$. The shape of the corresponding curves is very similar we see that the growth factor $D_1(a)$ only depends on h via its overall normalisation.

Approximation for the Growth Factor

An excellent approximation to the growth factor $D_1(a)$ of a flat universe ($\Omega_\Lambda = 1 - \Omega_m$) is given by

$$\frac{D_1(a, \Omega_m)}{D_1(a = 1, \Omega_m)} = \frac{5}{2}\Omega_m a \left[\Omega_m^{4/7} - \Omega_\Lambda + \left(1 + \frac{1}{2}\Omega_m\right)\left(1 + \frac{1}{70}\Omega_\Lambda\right)\right]^{-1}. \quad (3.13)$$

In Fig. 3.5 we show the growth factor from the simulation compared to this approximation. There is good agreement up to $a \sim 0.5$. This approximation is usually referenced to Carroll [4], although he gives further references to Lahav et al 1991 and Lightman & Schechter 1990.

3.3. The Power Spectrum Revisited

Now that we have seen the results of a cosmological constant Λ on the transfer function $T(k)$ and the growth factor $D_1(a)$ we are in a position to discuss the effects of Λ on the power spectrum. Fig. 3.6 shows the power spectrum in this model compared to the power spectrum that we discussed earlier. The spectrum of the model with Λ has been normalised to agree on large scales. The turnover point of this spectrum occurs for modes much larger then in the other model. The physical explanation for this is as follows: The model with Λ has a lot less matter ($\Omega_m = 0.3$) then the model without Λ, which implies that radiation-matter

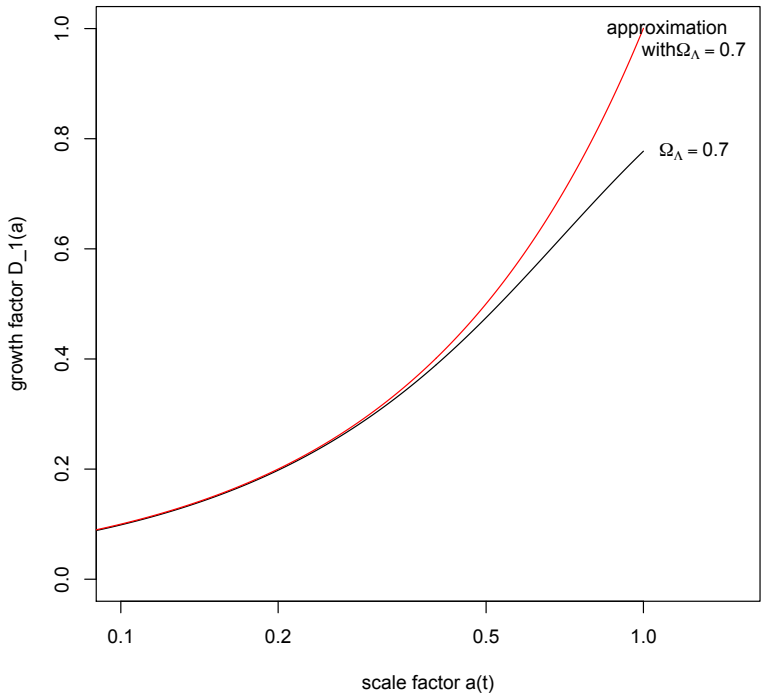

Figure 3.5.: The growth factor $D_1(a)$ of a flat model with Λ ($\Omega_m = 0.3, \Omega_\Lambda = 0.7$). The black line shows the growth factor obtained numerically, it is the same as in Fig. 3.3 and 3.4. The red line is the approximation of Eq. (3.13) with the parameters of this specific model. There is an excellent agreement up to $a \sim 0.5$.

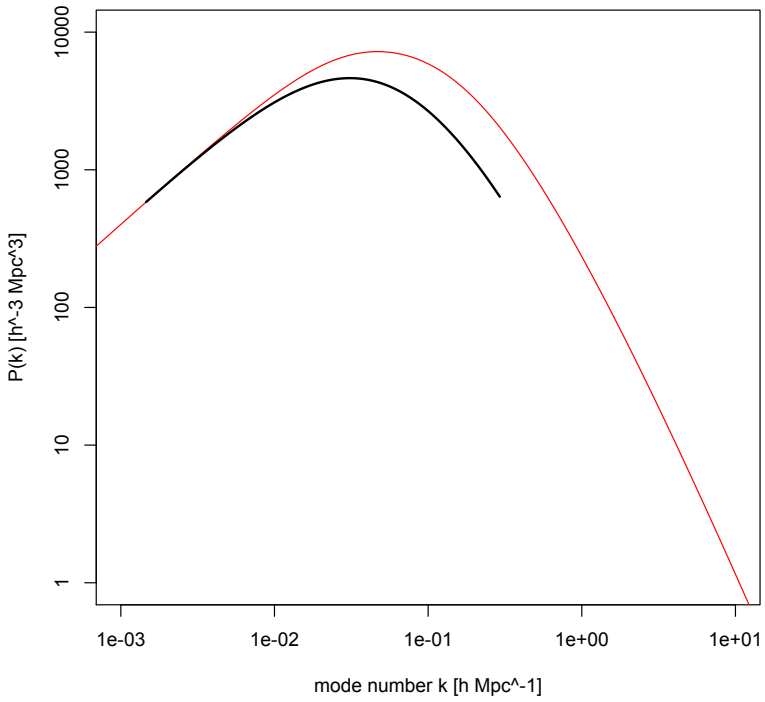

Figure 3.6.: Here the power spectrum obtained from the BBKS form of the transfer function (red line), c.f. Fig. 2.10, is compared to the power spectrum obtained from the simulation of the model with Λ. The spectra have been normalised to agree on large scales. The turnover point in the model with Λ is significantly earlier then in the model without. The small-scale modes are correspondingly more suppressed.

equality is correspondingly later. To see this we recall that the energy density of the photons is much higher then matter energy density, but falls off more rapidly, c.f. Fig. 1.2. This delay gives opportunity for more (i.e. larger) modes to enter the horizon during radiation domination or radiation-matter transition. These modes will experience suppressed growth due to radiation pressure and the turnover point in the power spectrum will thus occur on larger scales. A measurement of the power spectrum can thus be used to find the value of Ω_Λ.

3.4. Details of the Numerical Integration

We use the same numerical integrator as in the previous chapter. The one problem there is is the form of Eq. 7.77. It is an integral instead of a differential equation. However, we can easily convert this into a differential equation by taking the derivative with respect to a of this equation:

$$\frac{d}{da}\frac{D_1(a)}{H(a)} = \frac{5}{2}\Omega_m \frac{H_0^2}{(aH(a))^3}. \tag{3.14}$$

Recalling that the Friedmann equation in a universe with radiation, matter and dark energy is given by

$$\dot{a} = \frac{da}{d\eta} = H_0\sqrt{\Omega_r + \Omega_m a + \Omega_\Lambda a^4} \tag{3.15}$$

and that this can be used to cast the derivative with respect to a into a derivative with respect to η we see that

$$\frac{d}{d\eta}\frac{D_1(a)}{H(a)} = \frac{da}{d\eta}\frac{d}{da}\frac{D_1(a)}{H(a)} \tag{3.16}$$

$$= \frac{5}{2}\Omega_m H_0^2 \frac{\dot{a}}{(aH(a))^3}. \tag{3.17}$$

The differentiation with respect to $\log\eta$ then simply introduces another factor of η, just as before. H can be replaced using $aH = \dot{a}/a$ and the equation to be integrated then reads

$$\frac{d}{d\log\eta}\left(\frac{2}{5}\frac{1}{\Omega_m H_0^2}\frac{D_1(a)}{H(a)}\right) = \eta\,\frac{a^3}{\dot{a}^2}. \tag{3.18}$$

4. Dark Energy Equation of State: $p = w\rho$

The observational evidence for dark energy has grown immensely over the last decade. Whereas it was an open question whether the universe was accelerating or decelerating only fifteen years ago, today the evidence for an acceleration of the expansion of the universe is convincing. There are many review articles summarising the current indications that our universe has $\Omega_\Lambda \neq 0$, e.g. Eisenstein [6] or Bartelmann [3]. The literature agrees that the observations indicating dark energy are based on two pillars: Firstly, effects of dark energy on the scale factor $a(t)$, and secondly, on the growth of the perturbations (and in particular the matter inhomogeneities).

Supernovae Type Ia supernovae can be used as standard candles when their lightcurve is corrected in a well-studied manner. This is convincing although the physics of a supernova explosion is difficult to understand. Only recently have simulations started to reproduce the observed effects. In a flat universe we can thus infer the distance of those objects from the observed brightness and redshift. Ten years ago it was already known that distant supernovae appear to be too faint, e.g. Perlmutter [13].

Possible explanations range from mistakes in the physics of the supernovae to difficulties in the estimate of intergalactic absorption rates. The most striking explanation, however, is that the universe has recently undergone a phase of accelerated expansion. This would place these object a lot farther away and explain their apparent faintness. The observational basis that the latter explanation is the correct one has steadily grown ever since. It is a strong hint on its own for the existence of dark matter.

Acoustic Oscillations in the CMB The Cosmic Microwave Background (CMB) gives us a picture of the universe at very early times. Analysis shows that the angular correlations have a preferred scale of 1°. These oscillations give evidence for a nearly flat universe. They basically rule out an open, matter dominated

universe.

4.1. Inhomogeneities in case of $w \neq -1$

If dark energy behaves different from a cosmological constant, i.e. $w \neq -1$, it was pointed out by Pritchard, [15], that the growth factor can no longer be expressed as the integral

$$D_1(a) = \frac{5\Omega_m}{2} \frac{H(a)}{H_0} \int_0^a \frac{da'}{(a'H(a')/H_0)^3}. \tag{7.77}$$

Proof. To prove that for $w \neq -1$ Eq. (7.77) is no longer a solution to the differential equation for δ, Eq. (7.73), we insert it back. We see that it is a solution, if the Hubble rate $H(t)$ satisfies Eq. (7.73), i.e. if

$$\frac{d^2H}{da^2} + \left(\frac{d \log H}{da} + \frac{3}{a} \right) \frac{dH}{da} - \frac{3\Omega_m H_0^2}{2H^2 a^5} H = 0. \tag{4.1}$$

Dividing by H_0^2 and evaluating the differential of the logarithm we find that this is equivalent to

$$\frac{d^2}{da^2} \left(\frac{H^2}{H_0^2} \right) + \frac{3}{a} \frac{d}{da} \left(\frac{H^2}{H_0^2} \right) - 3\frac{\Omega_m}{a^5} = 0. \tag{4.2}$$

To see the implications of this equation we recall the Friedmann equation:

$$\frac{H^2}{H_0^2} = \Omega_r a^{-4} + \Omega_m a^{-3} + \Omega_k a^{-2} + \Omega_\Lambda. \tag{4.3}$$

The function on the left hand side is therefore a polynomial in a^{-1} To see that the Hubble rate fulfils this equation, we first see that the matter term $\Omega_m a^{-3}$ indeed fulfils it. We then try a power law ansatz: $H^2/H_0^2 = \Omega_m a^{-3} + \text{const} a^n$, where $n \in \mathbb{Z}$. The resulting terms do not violate Eq. (4.2) if

$$n^2 + 2n = 0 \quad \Leftrightarrow \quad \begin{cases} n = 0 & \text{or} \\ n = -2 \end{cases} \tag{4.4}$$

The first case corresponds to cosmological constant, the second to curvature. The radiation term is negligible in any case. This means that for general dark energy with $w \neq -1$ Eq. (7.77) cannot be true. □

A much more general treatment of the effects of dark energy is given for example in [12] or [9].

Conclusions

In this thesis we have demonstrated that small perturbations set at the end of inflation could be the source of the perturbations we observe today. Both, the theoretical as well as the numerical analysis of the evolution of inhomogeneities gives a consistent picture. The long period of matter domination is essential to explain the growth of the inhomogeneities. Although it is still not explained why Ω_Λ should be of the order of Ω_m, it is satisfying to see how well the physics of the evolution of perturbations agree with other aspects of physical cosmology like inflation, CMB and observations.

We have demonstrated how the power spectrum of matter inhomogeneities can be used to find the signature of dark energy in our universe. The controversy of what dark energy is and how it behaves is far from settled, and we have seen that the theory of a perturbed universe is right in the middle of it. The developments in the future will hopefully produce tighter observational bounds on transfer function and growth factor. Much better observational data can also be expected for the power spectrum. Combined they should provide us with very powerful tools to fix the position of our universe in the parameter space, and to determine the nature of dark energy.

A. Additional Notes and Calculations

A.1. Additional Formulae

The following integral is given in as entry 2.246 in Gradshteyn and Ryzhik, [8]: Let x be the variable of the integral, a, b, α and β arbitrary real parameter. Define then: $z := a + bx$, $t := \alpha + \beta x$ and $\Delta := a\beta - b\alpha$. Then, if $\beta\Delta > 0$, it is true that

$$\int \frac{dx}{t\sqrt{z}} = \frac{1}{\sqrt{\beta\Delta}} \log \frac{\beta\sqrt{z} - \sqrt{\beta\Delta}}{\beta\sqrt{z} + \sqrt{\beta\Delta}}. \tag{A.1}$$

B. Code

This appendix shows the components of the `C++` program used to simulate different models of the universe. This means that not all the code is shown that was used to create all the different figures throughout this document, but only the most important building blocks, i.e. functions, structures and classes used. We also do not include the `R`[1] code used to create the plots.

Furthermore, it does not contain the definitions and classes given in `Numerical Recipes`, [14]: In particular, we omit the class definitions of `nr3.h` and the `StepperDopr853` integrator mechanisms, but will provide a quick introduction:

The `StepperDopr853` routines integrate first order systems of the form

$$\dot{y} = \frac{dy}{dx} = f(x, y(x)), \tag{B.1}$$

where x is the 'time' variable of the system of differential equations, y the vector of components of the system. `StepperDopr853` then uses structure calls of the form

```
void operator() (const Doub x, VecDoub_I &y , VecDoub_O &dydx){...}
```

to find the values of $\dot{y} =$ `dydx` at position $(x, y) = (x, y(x))$. Organising the program in this way has the advantage that is it possible to change the system of differential equations without worrying about how to integrate it at the same time. The following pages will therefore contain many of these structures, each designed for a specific integration: the homogeneous background universe, the full Boltzmann-Einstein system or the integration of the growth factor are the most straightforward examples.

Parameters of the Models

We use the following set of overall parameters for the integration of the different systems:

```
const double H_0(h/2.99792458E3); // Hubble now in Mpc^-1
const double t_0(13.7/3.26156*1.0E3); // age of universe
                                      // again in Mpc
```

[1] http://www.r-project.org/

The parameters left for variability are h, k and the $\Omega_i, i = r, m, \Lambda$. They need to be set manually to the values of the model under consideration:

```
// parameter h for Hubble constant:
const double h(0.5);

// set the Omegas, the content of the universe:
const double Omega_m(0.3);
const double Omega_r(4.67E-5/h/h);
const double Omega_L(0.7-Omega_r);

// mode number k of the inhomogeneities:
// in units of h Mpc^-1
const double mode_k(0.001);
```

The Homogeneous Background

The differential equations for the background are core set of equations for all the differential systems we will be talking about. It is important for two reasons: First, it is the basic set of equations that drive the expansion of the universe. The radiation and matter perturbations will be put on top of that. Second, we always put a backwards integration first, in order to find the initial values for scale factor a, conformal time η and 'real' time t.

The following structure does exactly that by integrating in $\log \eta$:

```
struct cosmo_log{
Doub k,eta,a_dot;
cosmo_log(Doub kk): k(kk) {}
void operator() (const Doub logeta, VecDoub_I &y , VecDoub_O &
    dydx){
        // these are the differential equations
        //  ->          FORWARDS and BACKWARDS in eta

        eta = exp(logeta);

        // eqn for scale factor (integrate in log eta)
        a_dot = H_0*sqrt(Omega_m*y[0] + Omega_r +Omega_L*y[0]*y
            [0]*y[0]*y[0]);
        dydx[0] = eta*a_dot;

        // diff eqn for time t
        dydx[1] = eta*y[0]/t_0;
}  };
```

The Boltzmann-Einstein system

The next structure is used to integrate the full Boltzmann-Einstein system given by the equations (2.4) and the following on page 22.

```
struct cosmo_full{
Doub k, eta , a_dot, phi_dot;
cosmo_full(Doub kk): k(kk) {}
void operator() (const Doub logeta, VecDoub_I &y , VecDoub_O &
    dydx){
        // these are the differential equations:
        // ->          FORWARDS the FULL Boltzmann Einstein
            system

        eta = exp(logeta); // this set the \eta_0
        //  arbitrary normalization, but looks nice in the eta-
            scale plot.
        // also logeta =0  at time t=1year or a=10^-6

        // eqn for the scale factor (we integrate in log eta)
        a_dot = H_0*sqrt(Omega_m*y[0] + Omega_r +Omega_L*y[0]*y
            [0]*y[0]*y[0]);
        dydx[0] = eta*a_dot;

        // diff eqn for time t
        dydx[1] = eta*y[0]/t_0;

        // calculate phi_dot
        phi_dot = 1.0/3.0/a_dot*(1.5*H_0*H_0*(y[3]*Omega_m+4.0*y
            [5]*Omega_r/y[0])- y[0]*k*k*y[2]) - a_dot/y[0]*y[2];

        // eqn for potential phi then simply becomes
        dydx[2] = eta*phi_dot;

        // ------ the remaining equations ------
        // eqn for delta
        dydx[3] = eta*(-k*y[4]-3*phi_dot);

        // eqn for velocity
        dydx[4] = eta * (-a_dot/y[0]*y[4] -k*y[2]);

        // eqn for the monopole
        dydx[5] = eta*(-k*y[6]-phi_dot);

        // eqn for the dipole
        dydx[6] = eta*k/3.0*(y[5]-y[2]);
}  };
```

In the $\Omega_m = 1$ model the radiation perturbations are irrelevant to the structure formation. At some stage they can be safely ignored (c.f. the red line and discussion on page 34). This has been implemented in the following way:

```
struct cosmo_damp{
Doub k, eta , a_dot, phi_dot;
cosmo_damp(Doub kk): k(kk) {}
```

```
void operator() (const Doub logeta, VecDoub_I &y , VecDoub_O &
    dydx){
        // these are the differential equations:
        // ->          FORWARDS the DAMPED Boltzmann Einstein
            system

        eta = exp(logeta); // this set the \eta_0
        //  arbitrary normalization, but looks nice in the eta-
            scale plot.
        // also logeta =0  at time t=1year or a=10^-6

                // eqn for the scale factor (we integrate in log
                    eta)
        a_dot = H_0*sqrt(Omega_m*y[0] + Omega_r +Omega_L*y[0]*y
            [0]*y[0]*y[0]);
        dydx[0] = eta*a_dot;

        // diff eqn for time t
        dydx[1] = eta*y[0]/t_0;


        // calculate phi_dot (damping HERE)
        phi_dot = (1.0/3.0/a_dot*(1.5*H_0*H_0*(y[3]*Omega_m)- y
            [0]*k*k*y[2]) - a_dot/y[0]*y[2])*exp(-logeta*k/10.0)
            ;

        // eqn for potential phi then without eta (and HERE):
        dydx[2] =  phi_dot;

        // ------ the remaining equations -----
        // eqn for delta
        dydx[3] = eta*(-k*y[4]-3*phi_dot);

        // eqn for velocity
        dydx[4] = eta * (-a_dot/y[0]*y[4] -k*y[2]);

}       // radiation perturbations are blinded out
};
```

The Growth Factor $D_1(a)$

For the integration of the growth factor we use the same homogeneous background as before, but now equipped with the differential equation (3.18) from page 62:

```
struct cosmo_growth{
Doub k,eta,a_dot;
cosmo_growth(Doub kk): k(kk) {}
void operator() (const Doub logeta, VecDoub_I &y , VecDoub_O &
    dydx){
        // these are the differential equations:
        // ->          FORWARDS for the growth factor
```

```
8           eta = exp(logeta);

10          // eqn for the scale factor (we integrate in log eta)
            a_dot = H_0*sqrt(Omega_m*y[0] + Omega_r +Omega_L*y[0]*y
                [0]*y[0]*y[0]);
12          dydx[0] = eta*a_dot;

14          // diff eqn for time t
            dydx[1] = eta*y[0]/t_0;
16
            // diff eqn for the growth factor:
18          dydx[2] = eta/a_dot/a_dot*pow(y[0],3.0);
    }
20  };
```

The Core Parts of the Program

A very important function in the program is the function `doEvolve`. This function controls the initialising of the integration processes, their starts and stops. To do so it is called with some `flag` i to distinguish the output, the mode number k, the limits of the integrations ($\log(\eta_1)$ and $\log(\eta_2)$) and the vector y_{full} of initial values. The first part of the function initialises the output of the integration process into a file:

```
// doEvolve FUNCTION ---------------------------------
2 void doEvolve(int i,const double k, double logeta1, double
      logeta2,VecDoub yfull){
  // mode number k comes in units of h (Mpc)^-1
4
  // create the filename for the output:
6 stringstream myString;
  myString << "myfile" << i << ".csv";
8
  string bert = myString.str();    // convert it into a string
10// this needs to be converted into a char* by .c_str() see below

12// initialise writing in file:
  FILE * myfile;
14myfile = fopen(bert.c_str(), "w");
  fprintf(myfile, "header\t second\n");
16fprintf(myfile, "%f \t %f \t %f \t %f \t %f \t %f \n\n", Omega_m
      , Omega_r,Omega_L,k*factor, h, H_0*factor);

18// do the integrations:
  ...
20} };
```

After this the function starts the integration process, the lines omitted in the code above. In its simplest form this looks like:

```
// doing the integration in logeta of the full system:
        Output out2(-1);
        cosmo_full my_cosmoful(k);
        //h1=1.0E-4, hmin = 0.0;
        Odeint<StepperDopr853<cosmo_full> > ode2 (yfull,logeta1,
            logeta2,1.0E-18,1.0E-18,1.0E-4,0.0,out2,my_cosmoful)
            ;
        ode2.integrate();

        // then write in file
        for(int i = 0; i < out2.count; i++){
                fprintf(myfile, "%f \t %f \t %f \t %f \t %f \t %f \t
                    %f \t %f \n", out2.xsave[i], out2.ysave[0][i
                    ]*factor, out2.ysave[1][i]*factor,out2.ysave
                    [2][i]*factor,out2.ysave[3][i],out2.ysave
                    [4][i],out2.ysave[5][i],out2.ysave[6][i]);
        }
```

The problem here is that this function will not be able to consider the numerical difficulties when integrating small-scale modes at late times. The program will simply stop throwing an error message. However, we can instead integrate the full system only up to the red line in Fig. 2.4 and then restart it. The dots in the `doEvolve` function above are then to be replaced by the following code:

```
// calculate until when the full system can be evolved:
// for this use the if clause:
double x(log(100*k/h)*2.0/3.0);
std::cout << x << endl;

if (x<0){
        // doing the integration in logeta of the full system:
        Output out2(-1);
        cosmo_full my_cosmoful(k);
        //h1=1.0E-4, hmin = 0.0;
        Odeint<StepperDopr853<cosmo_full> > ode2 (yfull,logeta1,
            logeta2,1.0E-18,1.0E-18,1.0E-4,0.0,out2,my_cosmoful)
            ;
        ode2.integrate();

        // then write in file
        for(int i = 0; i < out2.count; i++){
                fprintf(myfile, "%f \t %f \t %f \t %f \t %f \t %f \t
                    %f \t %f \n", out2.xsave[i], out2.ysave[0][i
                    ]*factor, out2.ysave[1][i]*factor,out2.ysave
                    [2][i]*factor,out2.ysave[3][i],out2.ysave
                    [4][i],out2.ysave[5][i],out2.ysave[6][i]);
        }
} else {
```

```
19          // doing the integration in logeta of the full system
                until logeta2-x:
            Output out2(-1);
21          cosmo_full my_cosmoful(k);
            //h1=1.0E-4, hmin = 0.0;
23          Odeint<StepperDopr853<cosmo_full> > ode2 (yfull,logeta1,
                logeta2-x,1.0E-18,1.0E-18,1.0E-4,0.0,out2,
                my_cosmoful);
            ode2.integrate();
25
            // then integrate the damped system until today logeta2:
27          // but first find the new initial data:
            VecDoub yrestart(5); // five is the number of vars in
                the damped system!
29          yrestart[0] = out2.ysave[0][out2.count-1];
            yrestart[1] = out2.ysave[1][out2.count-1];
31          yrestart[2] = out2.ysave[2][out2.count-1];
            yrestart[3] = out2.ysave[3][out2.count-1];
33          yrestart[4] = out2.ysave[4][out2.count-1];

35          // then do the integration of the damped system:
            Output out3(-1);
37          cosmo_damp my_cosmodamp(k);
            //h1=1.0E-4, hmin = 0.0;
39          Odeint<StepperDopr853<cosmo_damp> > ode3 (yrestart,
                logeta2-x,logeta2,1.0E-18,1.0E-18,1.0E-4,0.0,out3,
                my_cosmodamp);
            ode3.integrate();
41
            // then write the first integration into the file
43          for(int i = 0; i < out2.count; i++){
                    fprintf(myfile, "%f \t %f \t %f \t %f \t %f \t
                        %f \t %f \n", out2.xsave[i], out2.ysave[0][i
                        ]*factor, out2.ysave[1][i]*factor,out2.ysave
                        [2][i]*factor,out2.ysave[3][i],out2.ysave
                        [4][i],out2.ysave[5][i],out2.ysave[6][i]);
45          }
            // then the second:
47          for(int i = 0; i < out3.count; i++){
                    fprintf(myfile, "%f \t %f \t %f \t %f \t %f \t %f \n
                        ", out3.xsave[i], out3.ysave[0][i]*factor,
                        out3.ysave[1][i]*factor,out3.ysave[2][i]*
                        factor,out3.ysave[3][i],out3.ysave[4][i]);
49          }
```

The `main` function of the program then only has to do the following:

- Evoke the integration backwards to find the initial values of the homogeneous background,
- Write the data into a file,

- Find the initial data of the full Boltzmann-Einstein system,
- Call the function `doEvolve`, possibly several times (in a `for`-loop)

Its code is given in the following:

```
// MAIN FUNCTION ----------------------------------------
int main (int argc, char * const argv[]) {

// the integration backwards for the homogeneous system:
VecDoub ylog(2);
ylog[0] = 1.0; // scale factor today
ylog[1] = 1.0; // time today

// doing the integration in logeta of the homogeneous system:
Output out_log(-1);
cosmo_log my_cosmolog(1.0); // ALWAYS CHECK THESE:
// if h=0.5 and Lambda start with 9.8668195 up to -3.0
// if h=0.73 and Lambda start with 9.497012 up to -4.0
// if h=0.5 and no Lambda start with 9.3783025 up to -3.0
Odeint<StepperDopr853<cosmo_log> > ode_log (ylog,9.497012,-3,1.0
    E-19,1.0E-19,1.0E-4,0.0,out_log,my_cosmolog);
ode_log.integrate();

// initialise writing in file for the backwards run:
FILE * pfile2;
pfile2 = fopen("myfile.csv", "w");

fprintf(pfile2, "header\t second\n");
fprintf(pfile2, "%f \t %f \t %f \t %f \t %f \t %f  \n\n", Omega_m
    , Omega_r,Omega_L,mode_k*factor, h, H_0*factor);

// write in file (
for(int i =0; i <out_log.count; i++){                    //
                    scale factor                                  time
        fprintf(pfile2, "%f \t %f \t %f \n", out_log.xsave[i],
            out_log.ysave[0][i]*factor, out_log.ysave[1][i]*
            factor);
}
// ----------------------
// so far so good
// ----------------------

// limits of the integration:
const Doub logeta1 = out_log.xsave[out_log.count-1];
// have found final value for eta
const Doub logeta2=  out_log.xsave[0];
// remember: cant do the full thing yet on small scales
// this means that logeta1 < logeta2 !

// THIS IS THE IMPORTANT LOOP THAT SCANS IN k
for (int i=0; i<1; i++) {
```

```
43 // set the MODE NUMBER k here:
   double k = mode_k*h*pow(1.4,1.0*i);
45 // note that the mode number k is given in Dodelson's units!!

47 // SET THE INITIAL VALUES OF THE FULL SYSTEM
   VecDoub yfull(7);
49
   // the values for the logeta integration
51 // initial value for the scale factor is last value of the
       backwards integration
   yfull[0] = out_log.ysave[0][out_log.count-1];
53 yfull[1] = out_log.ysave[1][out_log.count-1];

55 // a_dot in the beginning:
          Doub adot_start = H_0*sqrt(Omega_m*yfull[0] + Omega_r+
              Omega_L*pow(yfull[0],4.0));
57
   // potential phi (normalized from Fig. 7.2)
59 yfull[2] = pow(k,-1.5);
   // the other initial values depend on potential phi
61 yfull[3] = 1.5*yfull[2];
   yfull[4] = -0.5*k*yfull[2]*yfull[0]/adot_start;
63 yfull[5] = 0.5*yfull[2];
   yfull[6] = -k*yfull[2]*yfull[0]/6.0/adot_start;
65
   doEvolve(i,k, logeta1,logeta2, yfull);
67 }


69


71 return 0;
   }
```

Bibliography

[1] Supernova cosmology project: http://www-supernova.lbl.gov/.

[2] J. M. Bardeen, J. R. Bond, N. Kaiser, and A. S. Szalay. The statistics of peaks of gaussian random fields. *Astrophys. J.*, 304:15–61, May 1986.

[3] Matthias Bartelmann. The dark universe. *ArXiv e-prints, 0906.5036*, Jun 2009.

[4] Sean M. Carroll. The cosmological constant. *Ann. Rev. of Astronomy and Astrophysics*, 30:499–542, Apr 2000.

[5] Scott Dodelson. *Modern Cosmology*. Academic Press, 1st edition, March 2003.

[6] Daniel J Eisenstein. Observing dark energy. *Classical and Quantum Gravity*, 25(11):114001, 2008.

[7] W. L. Freedman, B. F. Madore, B. K. Gibson, L. Ferrarese, D. D. Kelson, S. Sakai, J. R. Mould, R. C. Kennicutt, Jr., H. C. Ford, J. A. Graham, J. P. Huchra, S. M. G. Hughes, G. D. Illingworth, L. M. Macri, and P. B. Stetson. Final Results from the Hubble Space Telescope Key Project to Measure the Hubble Constant. , 553:47–72, May 2001.

[8] I. S. Gradshteyn and I. M. Ryzhik. *Table of Integrals, Series and Products*. Elselvier, 7th edition, 2007.

[9] Wayne Hu and Daniel J. Eisenstein. Small-scale perturbations in a general mixed dark matter cosmology. *The Astrophysical Journal*, 498(2):497, 1998.

[10] Wayne Hu and Naoshi Sugiyama. Small-scale cosmological perturbations: An analytic approach. *The Astrophysical Journal*, 471(2):542, 1996.

[11] J. A. Peacock and S. J. Dodds. Nonlinear evolution of cosmological power spectra. *Mon. Not. R. Astron. Soc.*, 280:8, 1996.

[12] W. J. Percival. Cosmological structure formation in a homogeneous dark energy background. *A&A*, 443(3):819–830, 2005.

[13] S. Perlmutter, G. Aldering, G. Goldhaber, R. A. Knop, P. Nugent, P. G. Castro, S. Deustua, S. Fabbro, A. Goobar, D. E. Groom, I. M. Hook, A. G. Kim, M. Y. Kim, J. C. Lee, N. J. Nunes, R. Pain, C. R. Pennypacker, R. Quimby, C. Lidman, R. S. Ellis, M. Irwin, R. G. McMahon, P. Ruiz-Lapuente, N. Walton, B. Schaefer, B. J. Boyle, A. V. Filippenko, T. Matheson, A. S. Fruchter, N. Panagia, H. J. M. Newberg, and W. J. Couch. Measurements of omega and lambda from 42 high-redshift supernovae. *The Astrophysical Journal*, 517(2):565–586, Dec 1998.

[14] William Press, Saul Teukolsky, William Vetterling, and Brian Flannery. *Numerical Recipes in C*. Cambridge University Press, Cambridge, UK, 3rd edition, 2007.

[15] Jonathan Pritchard. On dodelson, exercise 7.11. http://home.fnal.gov/ dodelson/pritchard.pdf.

[16] Rimes, D. Christopher, Hamilton, and J. S. Andrew. Information content of the non-linear power spectrum: the effect of beat-coupling to large scales. *Monthly Notices of the Royal Astronomical Society*, 371(3):1205–1215, September 2006.